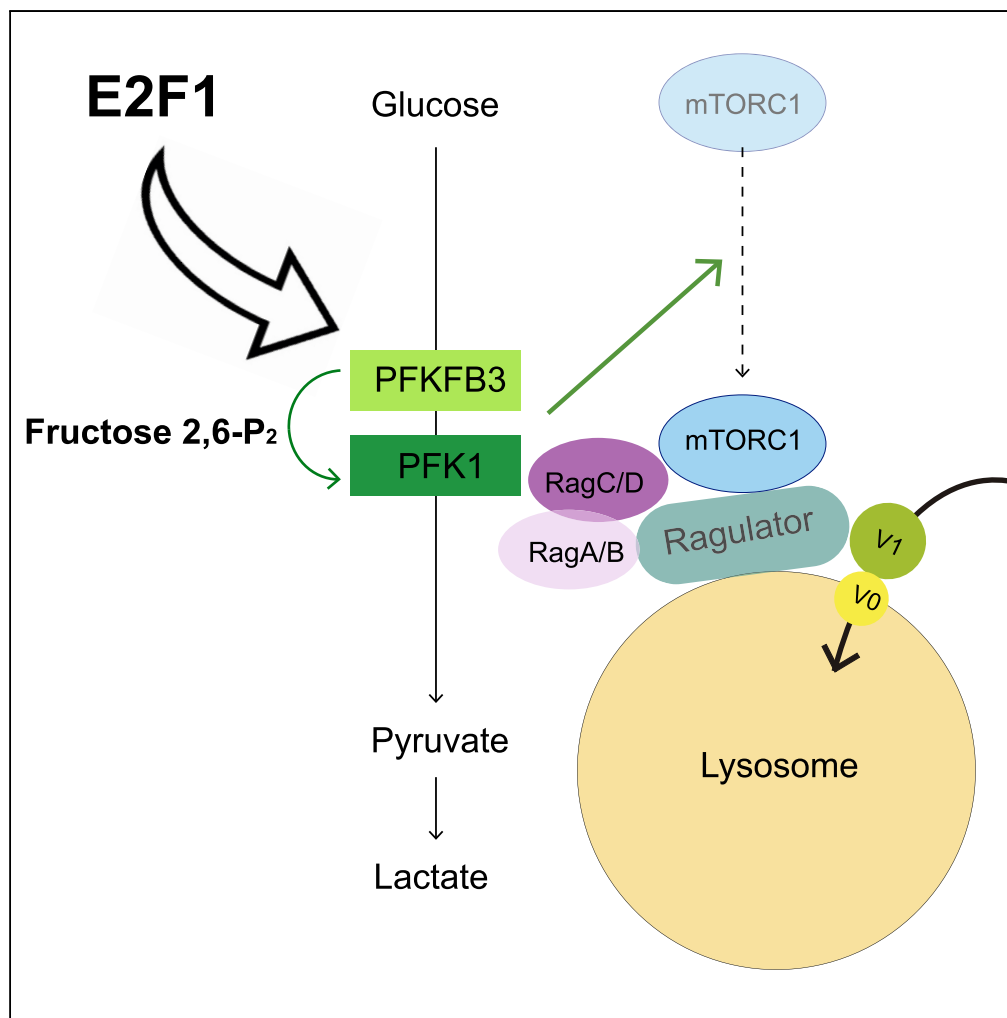**Article**

Phosphofructokinases Axis Controls Glucose-Dependent mTORC1 Activation Driven by E2F1

Eugènia Almacellas, Joffrey Pelletier, Anna Manzano, Antonio Gentilella, Santiago Ambrosio, Caroline Mauvezin, Albert Tauler

cmauvezin@idibell.cat (C.M.)
tauler@ub.edu (A.T.)

HIGHLIGHTS

Glucose potentiates E2F1-induced mTORC1 by promoting its translocation to lysosomes

PFKFB3 activity is involved in the regulation of mTORC1 by glucose

The glycolytic enzymes PFKFB3 and PFK1 were found associated to lysosomal surface

PFKFB3 and PFK1 activities regulate mTORC1 lysosomal translocation

Article

Phosphofructokinases Axis Controls Glucose-Dependent mTORC1 Activation Driven by E2F1

Eugènia Almacellas,[1,2] Joffrey Pelletier,[2] Anna Manzano,[3] Antonio Gentilella,[1,2] Santiago Ambrosio,[3] Caroline Mauvezin,[2,*] and Albert Tauler[1,2,4,*]

SUMMARY

Cancer cells rely on mTORC1 activity to coordinate mitogenic signaling with nutrients availability for growth. Based on the metabolic function of E2F1, we hypothesize that glucose catabolism driven by E2F1 could participate on mTORC1 activation. Here, we demonstrate that glucose potentiates E2F1-induced mTORC1 activation by promoting mTORC1 translocation to lysosomes, a process that occurs independently of AMPK activation. We showed that E2F1 regulates glucose metabolism by increasing aerobic glycolysis and identified the PFKFB3 regulatory enzyme as an E2F1-regulated gene important for mTORC1 activation. Furthermore, PFKFB3 and PFK1 were found associated to lysosomes and we demonstrated that modulation of PFKFB3 activity, either by substrate accessibility or expression, regulates the translocation of mTORC1 to lysosomes by direct interaction with Rag B and subsequent mTORC1 activity. Our results support a model whereby a glycolytic metabolon containing phosphofructokinases transiently interacts with the lysosome acting as a sensor platform for glucose catabolism toward mTORC1 activity.

INTRODUCTION

Metabolic reprogramming is considered one of the hallmarks of cancer (Pavlova and Thompson, 2016). To proliferate, cells must reach a critical size by promoting various anabolic processes required for growth, such as increased production of proteins, lipids, and nucleotides, and suppressing catabolic pathways like autophagy. In this context, mTORC1 has emerged as a major metabolic reprogramming node that controls the balance between anabolism and catabolism in response to environmental cues. mTORC1 signaling promotes protein synthesis largely through the phosphorylation of two key effectors, p70S6 Kinase 1 (S6K1) and eIF4E Binding Proteins (4EBPs). Moreover, mTORC1 enhances biosynthesis of lipids as well as nucleotide precursors, which are required to expand membranes and to generate nucleotides for RNA and DNA synthesis (Saxton and Sabatini, 2017).

Cancer cells depend on mTORC1 activity to couple mitogenic signaling with nutrients availability for growth. Growth factors induce mTORC1 mainly through the TSC/Rheb canonical pathway. Activation of PI3K/Akt and Ras/MAPK pathways by mitogens converge on the phosphorylation and inhibition of Tuberous Sclerosis Complex 2 (TSC2), a GTPase-activating protein (GAP) for the G-protein Rheb. Upon growth factor stimulation, TSC phosphorylation results in its dissociation from the lysosomal surface where Rheb is localized leading to GTP-bound Rheb accumulation and consequent mTORC1 activation (Inoki et al., 2002; Ma et al., 2005; Menon and Manning, 2008; Oki et al., 2005). Given that several components within these pathways are oncogenes or tumor suppressors, deregulation of the TSC/Rheb axis is the main mechanism attributed to oncogenic transformation for controlling mTORC1 activity. However, despite this general agreement, some oncogenes use alternative pathways to regulate mTORC1 activity and cell growth such as E2F1 or c-Myc (Meo-Evoli et al., 2015; Pourdehnad et al., 2013).

In contrast to mitogenic signaling, amino acids control mTORC1 by regulating Rag GTPases activity that promotes the translocation of mTORC1 to the lysosomal surface where it can be activated by Rheb (Bar-Peled et al., 2012; Kim et al., 2008; Sancak et al., 2010). Rag GTPases consist of constitutive Rag A or B and Rag C or D heterodimers, with GTP-bound Rag A or B being the active form. Several studies show that amino acids control the nucleotide loading state of Rag GTPases by promoting the GEF activity of the Ragulator complex (Wolfson and Sabatini, 2017). Although the precise mechanism by which amino

[1]Department of Biochemistry and Physiology, School of Pharmacy, University of Barcelona, Barcelona, Catalonia 08028, Spain

[2]Laboratory of Cancer Metabolism, Molecular Mechanisms and Experimental Therapy in Oncology Program (Oncobell), Institut d'Investigació Biomèdica de Bellvitge (IDIBELL), Hospitalet del Llobregat, Barcelona, Catalonia 08908, Spain

[3]Biochemistry Unit, Physiological Sciences Department, Faculty of Medicine and Health Science, University of Barcelona (IDIBELL), Hospitalet del Llobregat, Catalonia 08907, Spain

[4]Lead Contact

*Correspondence: cmauvezin@idibell.cat (C.M.), tauler@ub.edu (A.T.)

https://doi.org/10.1016/j.isci.2019.09.040

acids regulate Ragulator is still unclear, the vacuolar H$^+$-adenosine triphosphatase ATPase (v-ATPase) activity is essential for this process (Zoncu et al., 2011). Regulation of v-ATPase by nutrients controls Ragulator GEF activity toward the Rag GTPases, inducing the translocation of mTORC1 to lysosomes and its activation.

Recent studies demonstrate that v-ATPase activity is a key step for the activation of mTORC1 by the E2F1 oncogene. E2F1 activates mTORC1 by transcriptional regulation of the v-ATPase subunit, ATP6V0B (Meo-Evoli et al., 2015; Real et al., 2011). The E2F1 transcription factor is overexpressed in numerous human cancers, including lung, breast, and hepatocellular carcinomas, as well as Sporadic Burkitt Lymphomas (Eymin et al., 2001; Ladu et al., 2008; Molina-Privado et al., 2009; Zhang et al., 2000). Consistent with this observation, tumors from transgenic mice in which E2F1 is overexpressed possess high mTORC1 activity, suggesting that the effects of E2F1 on tumorigenesis may be in part mediated by mTORC1 (Ladu et al., 2008).

Essential for their survival, most tumor cells take up more glucose than normal cells resulting in an increase on aerobic glycolysis, a phenomenon known as the Warburg effect (Warburg, 1956). Accordingly, activation of oncogenes such as Ras, Akt, or c-Myc or loss of tumor suppressor genes such as p53 promote glucose uptake and lactate production (Bensaad et al., 2006; Gordan et al., 2007; Manning and Cantley, 2007; Ramanathan et al., 2005). In this regard, it has been shown that E2F1 can promote a metabolic switch by both, enhancing aerobic glycolysis and repressing mitochondrial oxidation (Denechaud et al., 2017). In proliferative situations, E2F1 transcriptionally activates the expression of the F-type isoform of the glycolytic enzyme, 6-phophofructo-2-kinase/fructose-2,6-bisphosphatase (PFK/FBPase) (Darville et al., 1995). Moreover, in hepatocellular carcinoma cells, expression of several glycolytic enzymes genes is enhanced by E2F1-induced Pontin/Reptin helicases complex recruitment to E2F target genes. In bladder and prostate cancer cell lines, E2F1 also increases glycolysis through the suppression of Sirtuin 6 expression (Tarangelo et al., 2015; Wu et al., 2015). In parallel, E2F1 inhibits mitochondrial oxidation by enhancing the expression of pyruvate dehydrogenase kinases (PDKs) 1 and 3 genes (Wang et al., 2016).

Considering the metabolic function of E2F1, we hypothesize that glucose catabolism driven by E2F1 could participate in mTORC1 activation. In this work, we demonstrate that E2F1-dependent mTORC1 activation relies on glucose availability and identify the key regulatory enzymes, PFKFB3 and PFK1, as proteins that interact with the lysosomal surface and regulate mTORC1 activity. These results support a model whereby a glycolytic metabolon containing phosphofructokinases act at the lysosome as a sensor platform for glucose metabolism toward mTORC1 activity.

RESULTS

Glucose Potentiates E2F1-Induced mTORC1 Activation by Promoting Its Translocation to Lysosomes

As glucose is the main nutritional source for the maintenance of cancer cells growth, we investigated the importance of glucose for mTORC1 activation under E2F1 oncogenic signaling (Warburg, 1956). To model oncogene-induced cell growth, we used the previously reported U2OS ER-E2F1 stable cell line that allows the control of E2F1 transcriptional activity by the addition of 4-hydroxitamoxifen (OHT) (Agger et al., 2005; Real et al., 2011). To validate the system, cells were serum starved to minimize the activity of endogenous E2F1 and treated or not with OHT. E2F1-target genes (Cyclin E and Bcl-2) mRNA expression was analyzed by quantitative RT-PCR to evaluate E2F1 transcriptional activation. As expected, OHT treatment induced an increase in E2F1-target genes mRNA (Figure S1A). To evaluate the implication of glucose on E2F1-induced mTORC1 activation, cells were glucose starved or not before E2F1 induction (OHT) and mTORC1 activity was analyzed by the phosphorylation of its downstream targets p70S6 kinase (pS6K T389) and S6 (pS6 S235/236). Glucose starvation induced a dramatic reduction of mTORC1 activity both in control and E2F1-induced cells. Additionally, E2F1-induced mTORC1 activation was not significant in glucose-starved cells, whereas glucose addition significantly enhanced mTORC1 activation by E2F1 (Figures 1A and 1B). To discard any effect of OHT treatment independent of E2F1 activation, U2OS wild-type cells were treated under the same experimental conditions. Our results showed no effect of OHT on mTORC1 activation either with or without glucose presence (Figure S1B). As glucose deprivation affects energetic balance, we analyzed AMPK activity by measuring its auto-phosphorylation (pAMPK T172) as well as the phosphorylation of its downstream target Acetyl-CoA Carboxylase (pACC S79). As expected, glucose-starved cells displayed an increased AMPK activity (Figure 1A). However, E2F1 induction did not alter either AMPK or ACC phosphorylation, indicating that E2F1-induced mTORC1 activation is independent of AMPK (Figure 1A). Similar results were obtained in HeLa cells transiently expressing ER-E2F1
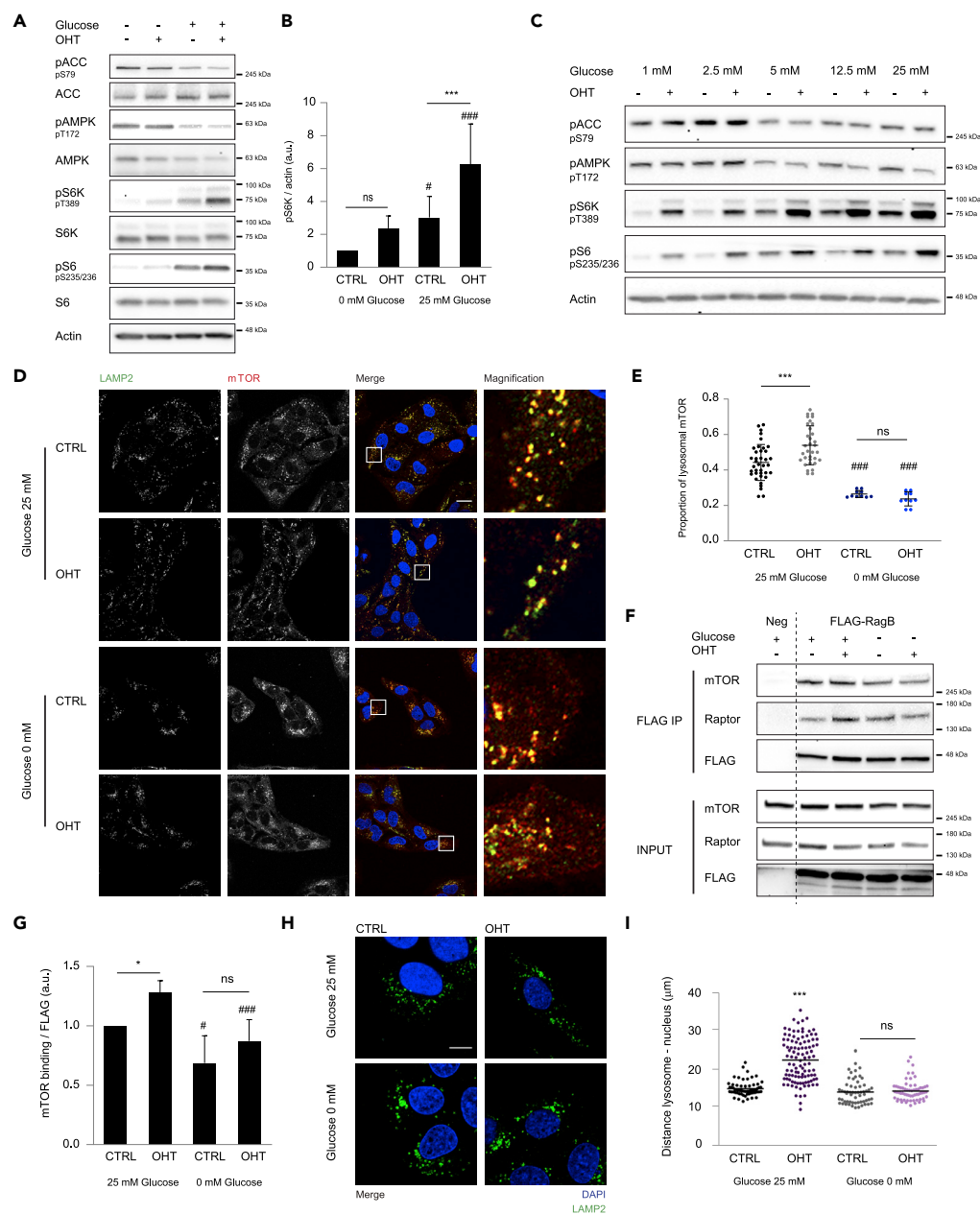
Figure 1. Glucose Is Required for Maximum E2F1-Induced mTORC1 Activation and Lysosomal Localization

(A) U2OS ER-E2F1 cells were serum starved overnight, cultured in the presence (25 mM) or absence (0 mM) of glucose for 1 h before OHT treatment for 6 h. Indicated proteins were analyzed by western blot. β-Actin was used as a loading control.

(B) Intensity of S6K phosphorylation was analyzed in n = 7 independent experiments and normalized to β-actin band intensity.

(C) U2OS ER-E2F1 cells were serum starved overnight, cultured in increasing concentrations of glucose (1–25 mM) for 1 h before OHT treatment for 6 h. Indicated proteins were analyzed by western blot. β-Actin was used as a loading control.

(D) U2OS ER-E2F1 cells were treated as described in (A), and mTOR (red) and LAMP2 (green) were analyzed by Immunofluorescence analysis under indicated experimental conditions. DAPI (blue) was used to stain the DNA. Scale bar corresponds to 10 μm.

(E) Quantification of lysosomal mTOR under experimental conditions of (D) (red pixels co-localizing with green pixels compared with total red pixels).

(F) U2OS ER-E2F1 cells were serum starved overnight, cultured in the presence (25 mM) or absence (0 mM) of glucose for 1 h before OHT treatment for 6 h. FLAG-Rag B was immunoprecipitated under indicated experimental conditions, and

Figure 1. *Continued*

indicated proteins were analyzed by western blot. U2OS ER-E2F1 cells were used as a negative control for the immunoprecipitation.

(G) Band intensities of mTOR normalized by FLAG intensity was measured and plotted in n = 5 independent immunoprecipitation experiments.

(H) Representative confocal images of U2OS ER-E2F1 serum starved overnight, glucose starved or not for 1 h before OHT treatment for 6 h. LAMP2 (green) was used to detect lysosomes and DAPI (blue) to stain the DNA. Scale bar corresponds to 10 μm.

(I) Quantification of lysosome-nucleus distance based on single-cell analysis.

Data are presented as mean ± SD. Statistical significance is shown as: *p < 0.05; **p < 0.005; ***p < 0.001 for OHT effect compared with CTRL and #p < 0.05; ##p < 0.005; ###p < 0.001 for effect of glucose compared with the respective control; ns: p > 0.05. See also Figure S1.

fusion protein indicating that the response is not cell-type dependent (Figure S1C). Cyclin E expression was used for the validation of the E2F1 induction in these cells (Figure S1C). To discard a time-dependent response, AMPK activity was analyzed at different times upon E2F1 induction. Neither AMPK auto-phosphorylation nor the phosphorylation of its down-stream targets (pRaptor S792, pULK1 S555, pACC S79) was affected after 2 to 6 h of E2F1 induction, whereas mTORC1 was progressively activated as shown by the time-dependent increase of S6K phosphorylation (Figure S1D). E2F1-induced mTORC1 activation was complementary analyzed at increasing glucose concentrations. Interestingly, the kinetics of mTORC1 activation did not follow AMPK activity (Figure 1C). Although AMPK shows a bimodal activity, being either highly phosphorylated in low glucose (1–2.5 mM) or slightly phosphorylated in high glucose (5–25 mM), mTORC1 activity concomitantly increases with glucose concentration from 5 to 25 mM (Figures 1C and S1E). In high glucose conditions, the slope of mTORC1 activation was higher in E2F1-induced cells than in control cells showing the importance of this nutrient for E2F1-dependent mTORC1 activation, whereas AMPK activity remained constant in both situations (Figure S1E). Our results suggest that, although AMPK plays a role in glucose sensing toward mTORC1, other parallel mechanisms independent of AMPK activity are involved on transducing glucose availability to mTOR. To finally validate the effect of E2F1 directly on the energetic balance, adenine nucleotides levels were analyzed by Ultra Performance Liquid Chromatography, which showed no major changes either in global ATP/ADP/AMP levels or in the AMP/ATP ratio or Energy Charge (Figures S1F–S1H). Altogether, our results here support that glucose potentiates E2F1-induced mTORC1 activity independently of AMPK.

Translocation of mTORC1 to lysosomes was proposed to be crucial for E2F1-driven mTORC1 activation (Meo-Evoli et al., 2015). To test whether glucose participates in this process, mTORC1 recruitment to LAMP2-positive lysosomes was quantified in the absence or presence of glucose by immunofluorescence analysis. The portion of endogenous lysosome-localized mTORC1 was around 40% in control cells and rose to 60% upon E2F1 induction (Figures 1D and 1E). However, absence of glucose reduced mTORC1 lysosomal localization in control and E2F1-induced cells (Figures 1D and 1E). Importantly, this result was consistent in HeLa cells transiently expressing ER-E2F1 (Figures S1I and S1J). Since mTORC1 translocation to the lysosome is mediated by the Rag GTPases, we evaluated the effect of glucose on mTORC1 binding to Rag B. Using the previously established Rag B-FLAG ER-E2F1 U2OS stable cells (Meo-Evoli et al., 2015), we analyzed the interaction between mTORC1 components (mTOR and Raptor) and Rag B by FLAG immunoprecipitation. mTOR and Raptor association to Rag B was enhanced in glucose-rich conditions and potentiated by E2F1 induction, whereas glucose starvation reduced the affinity of mTORC1 to Rag B both in control and E2F1-induced cells (Figures 1F, 1G, and S1K). Overall, these results show that glucose enhances the translocation of mTORC1 to lysosomes and is essential for E2F1-induced mTORC1 lysosomal localization.

Cellular distribution of lysosomes has been associated with the recruitment and activity of mTORC1 (Korolchuk et al., 2011). Accordingly, we previously showed that E2F1 activation induced lysosomal trafficking from perinuclear distribution toward the cell periphery (Meo-Evoli et al., 2015). By image-based single-cell analysis, we measured the effect of glucose on the distance between individual lysosomes and the center of the nucleus. Glucose starvation abolished lysosomal peripheral distribution induced by E2F1, without significantly affecting lysosome localization in control cells, suggesting an essential role of glucose in E2F1-driven lysosomal trafficking (Figures 1H and 1I).

E2F1 Induces Glycolysis

Given that E2F1 effect on mTORC1 activation is independent of energy charge but connected to glucose availability, we studied the involvement of glucose catabolism on E2F1-induced mTORC1 activation. To

this end, mTORC1 activity was analyzed upon E2F1 induction in cells treated either with 2-deoxyglucose (2DG), which blocks glycolysis, and/or Oligomycin A (Oligo A), which inhibits the mitochondrial H^+-ATP synthase. Although in control cells both 2DG and Oligo A inhibited mTORC1 activity to the same extent, E2F1 was unable to significantly activate mTORC1 specifically upon 2DG treatment (Figures 2A and 2B). Notably, the capacity of E2F1 to induce mTORC1 activation tended to increase after impairing mitochondrial oxidation with Oligo A (Figures 2A and 2B). The combination of both reagents completely blocked mTORC1 activity in both control and E2F1-induced cells. Overall, these results suggest that E2F1-induced mTORC1 activation depends on the glycolytic flux. In parallel, mTORC1 lysosomal recruitment was assessed by co-immunofluorescence of mTOR and LAMP2, showing a reduction of lysosomal mTOR fraction upon glycolysis blockade by 2DG in E2F1-induced cells (Figures 2C and 2D).

Since E2F1 was previously identified as a regulator of glucose metabolism, we investigated whether E2F1 was able to induce glycolysis in our system (Blanchet et al., 2011). Hence, we measured in real time the extracellular acidification rate (ECAR), as indicator of lactic acid production in U2OS cells by SeaHorse GlycoStress analysis. E2F1-induced cells displayed an increased ECAR in glucose-stimulated (basal glycolysis) and Oligo A-treated conditions (maximum glycolysis) validating that E2F1 enhances glycolysis in this model (Figures 2E–2G). In parallel, mitochondrial oxidation was measured by Oxygen Consumption Rate, showing that both processes are indeed induced by E2F1 (Figures S2A and S2B). As mTORC1 has been shown to induce glycolysis, we tested whether the E2F1 effect on glycolysis induction was attributable to mTORC1 (Moon et al., 2015). To this end, E2F1-induced glycolysis was measured in the presence of mTORC1 allosteric inhibitor RAD001, combined with the ATP-site competitive inhibitor BEZ235 to completely block mTOR activity as previously shown (Thomas et al., 2012). As expected, mTORC1 inhibition induced a robust decrease in both basal and maximum glycolysis (Figures 2H, S2C, and S2D). However, even under these conditions, E2F1 increased the glycolytic flux, demonstrating that E2F1-driven glycolysis does not rely on mTORC1 activation (Figures 2H, S2C, and S2D).

Aerobic glycolysis products such as protons and lactate need to be extruded to prevent cytosolic acidification and consequent toxicity. To assess whether E2F1 is able to regulate the transport of cytosolic protons in parallel to glycolysis induction, cytosolic pH was determined by staining cells with the permeable SNARF-AM ester, which specifically emits fluorescence when internalized in a pH-sensitive manner. E2F1 activation provoked the alkalinization of the cytosol (Figure 2I). In parallel, we studied the expression of different proton transporters upon E2F1 induction and found that at least the monocarboxylate transporters (MCTs) MCT1 and MCT4 and the carbonic anhydrase CA2 mRNA levels were enhanced by E2F1 (Figures S3A–S3C). However, down-regulation of MCT1 was not sufficient to counteract cytosolic alkalinization induced by E2F1 (Figure S3D). Of note, depletion of MCT1 transporter activates a compensatory mechanism resulting in an increase in the mRNA levels of both MCT4 and CA2 (Figures S3B and S3C). Overall these results demonstrate that E2F1 regulates glucose metabolism by increasing aerobic glycolysis and intracellular pH.

The molecular mechanism by which E2F1 drives glycolysis might be broad, as this transcription factor has been proposed to regulate more than 30% of the human genome (Bieda et al., 2006). From public gene expression database (GEO: GSE39136), we identified potential glycolytic targets that could account for the effect of glucose on E2F1-induced mTORC1 activation (Shats et al., 2013). Results of this analysis pointed out that mRNA levels of the PFK/FBPase isoform 3 (PFKFB3) significantly increased upon E2F1 induction (Figures 3A and 3B). We validated this result by quantitative RT-PCR and at protein level (Figures 3C–3E). PFK/FBPase is a well-known bifunctional enzyme responsible of Fructose 2,6-P_2 metabolism, an allosteric activator of the rate-limiting glycolytic enzyme, ATP-dependent 6-phosphofructokinase (PFK1) (Pilkis et al., 1981). To confirm that the increase on PFKFB3 expression upon E2F1 induction leads to an increase in its activity, Fructose 2,6-P_2 levels were measured by an enzymatic assay as previously described (Van Schaftingen et al., 1982). Effectively, E2F1 induction led to a 15% increase in Fructose 2,6-P_2 levels, suggesting that PFKFB3 action could occur through PFK1 allosteric regulation (Figure 3F). To validate that E2F1-dependent PFKFB3 up-regulation is not cell-type specific, we analyzed PFKFB3 expression upon E2F1 induction in HeLa cells transiently overexpressing ER-E2F1. Accordingly, PFKFB3 protein levels were increased upon E2F1 induction (Figure 3G).

PFKFB3 Regulates E2F1-Driven mTORC1 Activity

The fact that E2F1 induces PFKFB3 expression raises the possibility that this isoenzyme mediates the E2F1-driven mTORC1 activity. To test this hypothesis, we evaluated mTORC1 activity after chemical and genetic
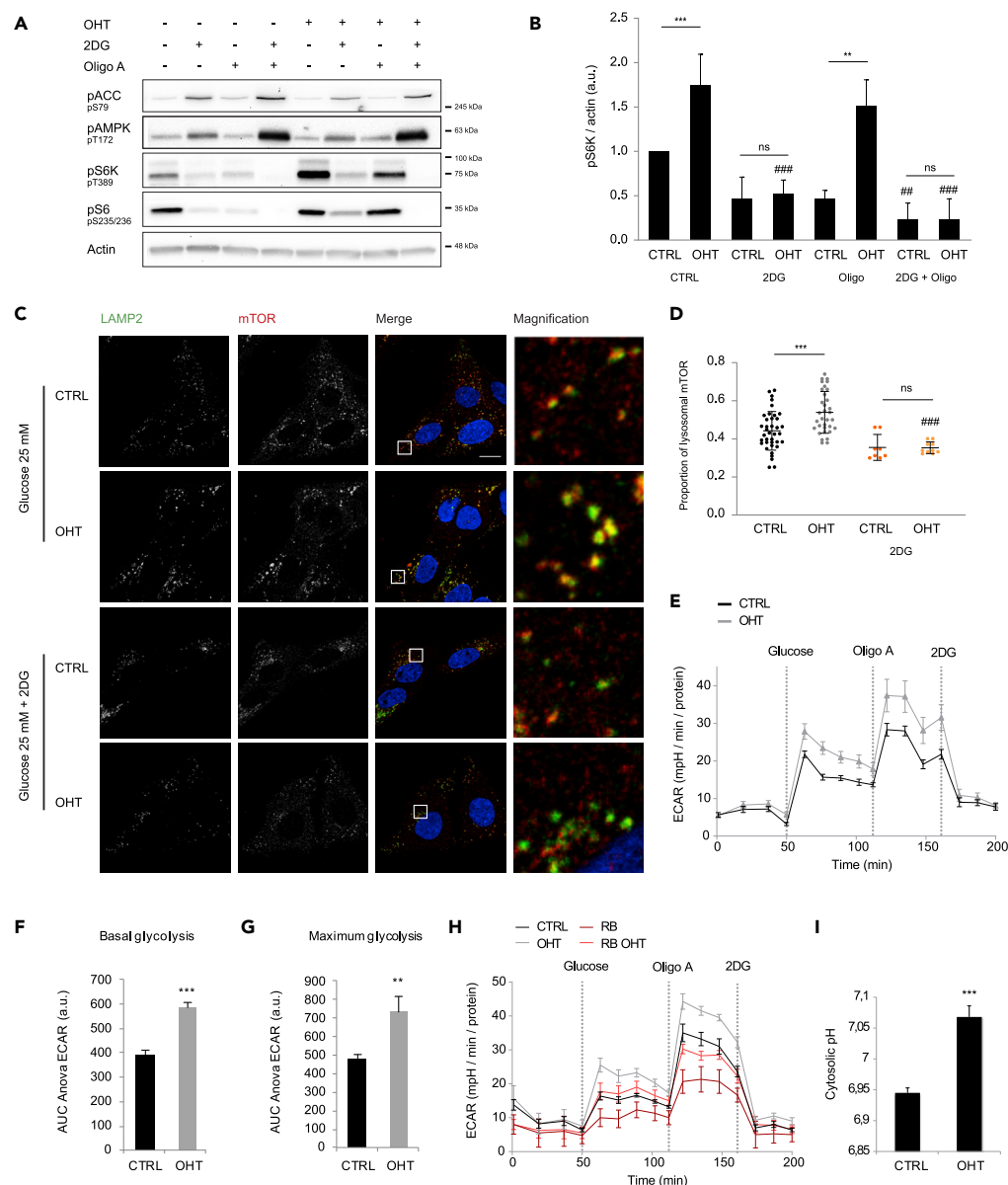
Figure 2. E2F1-Induced mTORC1 Activation Requires Glycolysis

(A) U2OS ER-E2F1 cells were serum starved overnight, treated with 2-deoxyglucose (2DG) and/or Oligomycin A (Oligo A) for 1 h before OHT treatment for 6 h. Indicated proteins were analyzed by western blot. β-Actin was used as a loading control.

(B) Intensity of S6K phosphorylation was analyzed in n = 3 independent experiments and normalized to β-actin band intensity.

(C) Cells were serum starved overnight and subjected to the indicated treatments for 1 h before OHT treatment for 6 h. mTOR (red) and LAMP2 (green) were identified by immunofluorescence analysis. Scale bar corresponds to 10 μm.

(D) Quantification of lysosomal mTOR under experimental conditions of (C) (red pixels co-localizing with green pixels compared with total red pixels).

(E) U2OS ER-E2F1 cells were treated or not with OHT for 6 h and subjected to SeaHorse analysis. Representative GlycoStress Test result is shown for n = 3 independent experiments.

(F) Area Under the Curve (AUC) analysis from glucose to Oligo A injections indicating the glucose-stimulated glycolytic capacity (basal glycolysis).

(G) Area Under the Curve (AUC) analysis from Oligo A to 2DG injections indicating the maximum glycolytic capacity.

(H) U2OS ER-E2F1 cells were treated or not with OHT for 6 h in presence or absence of RAD001 + BEZ235 (RB) and subjected to SeaHorse analysis. Representative GlycoStress Test result is shown for n = 3 independent experiments.

Figure 2. Continued

(I) U2OS ER-E2F1 cells were serum starved overnight and treated with OHT for 16 h. SNARF-AM ester was used to determine cytosolic pH based on standard curve with adjusted pH.

Data are presented as mean $\pm$ SD. Statistical significance is shown as: *$p < 0.05$; **$p < 0.005$; ***$p < 0.001$; ns: $p > 0.05$. See also Figures S2 and S3.

inhibition of PFKFB3. Treatment with the specific PFKFB3 inhibitor (3-pyridinyl)-1-(4-pyridinyl)-2-propen-1-one (3PO) significantly impaired E2F1-induced mTORC1 activity as well as basal levels (Figures 4A and 4B) (Clem et al., 2008). Furthermore, inhibition of PFKFB3 activity by 3PO also led to decreased mTORC1 activity in HeLa cells, indicating that this regulation is not restricted to the U2OS cell line (Figure S4A). To exclude side effects of the drug, PFKFB3 genetic depletion was performed by small interfering RNA. As expected, siPFKFB3 also led to decreased mTORC1 activity, specifically in E2F1-induced cells, indicating a potential role of this enzyme in regulating mTORC1 activity (Figures 4C and 4D). To evaluate the importance of Fructose 2,6-P_2 levels on E2F1-induced mTORC1 activation, we overexpressed the tumor suppressor gene TP53-induced glycolysis and apoptosis regulator (TIGAR). Expression of TIGAR has been reported to decrease Fructose 2,6-P_2 levels owing to its fructose-2,6-bisphosphatase activity (Bensaad et al., 2006). TIGAR overexpression led to a reduction in mTORC1 activity in all tested conditions (Figures 4E and 4F) corroborating that PFKFB3 action on mTORC1 occurs by modulating Fructose 2,6-P_2 levels. Of note, AMPK phosphorylation was not affected by any of these treatments indicating that mTORC1 regulation is independent of AMPK regulation (Figures 4A, 4C, and 4E). To validate the effect of these treatments on Fructose 2,6-P_2, metabolite levels were monitored confirming its reduction after chemical and genetic inhibition of PFKFB3 as well as after TIGAR overexpression (Figure 4G). Noteworthy, glucose starvation also reduced Fructose 2,6-P_2 levels unveiling the possible role of this metabolite on glucose-mediated mTORC1 regulation (Figure 4G).

We further examined whether PFKFB3 expression was sufficient to induce mTORC1 activity (Duran et al., 2008). PFKFB3 overexpression produced a striking increase of mTORC1 activity in E2F1-induced and non-induced cells to the same extent (Figures 4H and 4I). As expected, Fructose 2,6-P_2 levels increased upon PFKFB3 overexpression (Figure 4J). Overall, these results demonstrate that E2F1 regulates PFKFB3 expression and by this mechanism controls mTORC1 activation.

As Fructose 2,6-P_2, the PFKFB3 catalytic product, is an allosteric regulator of the rate-limiting glycolytic enzyme, PFK1, we evaluated its involvement in E2F1-induced mTORC1 activity. Depletion of the three PFK1 isoforms (PFKL, PFKP, PFKM) by small interfering PFK1 RNA mix (siPFK1) induced a slight but significant decrease of S6K, suggesting the implication of PFK1 on E2F1-driven mTORC1 activation (Figures 4K and 4L). PFK1 protein was still detected by western blot, suggesting that part of the remaining mTORC1 activity could be due to PFK1 partial depletion (Figure 4K). Interestingly, E2F1-induced mTORC1 activity was not inhibited upon depletion of PFK1 downstream glycolytic enzymes Aldolase or GAPDH (Figures S4B and S4C), indicating that regulation of mTORC1 activity occurs at the PFK axis. These results suggest that PFKFB3 regulates mTORC1 activity through allosteric modulation of PFK1 activity.

PFKFB3 Regulates mTORC1 Lysosomal Translocation

As glucose is essential for mTORC1 lysosomal translocation, we investigated the implication of PFKFB3 on mTORC1 lysosomal localization. To this end, mTORC1 recruitment to LAMP2-positive lysosomes was quantified by immunofluorescence analysis of mTOR and LAMP2 colocalization after PFKFB3 modulation. PFKFB3 overexpression increased lysosomal mTORC1 localization on E2F1-induced and non-induced cells (Figures 5A and 5B). Inhibition of PFKFB3 activity by 3PO resulted in a reduction of mTORC1 localized in LAMP2-positive lysosomes in both E2F1-induced and non-induced cells (Figures 5A and 5B). Similar reduction on mTORC1 lysosomal localization was obtained upon PFKFB3 genetic depletion by small interfering RNA (Figures S5A and S5B). To note, E2F1-induced mTORC1 lysosomal translocation was similarly reduced by PFKFB3 chemical inhibition in HeLa cells transiently expressing ER-E2F1 (Figures S5C and S5D).

Since mTORC1 translocation to the lysosome is mediated by the Rag GTPases, we evaluated the effect of PFKFB3 inhibition on mTORC1 binding to Rag B. FLAG-Rag B immunoprecipitation analysis showed that recruitment of both, mTOR and Raptor, was reduced in 3PO-treated cells, confirming the role of
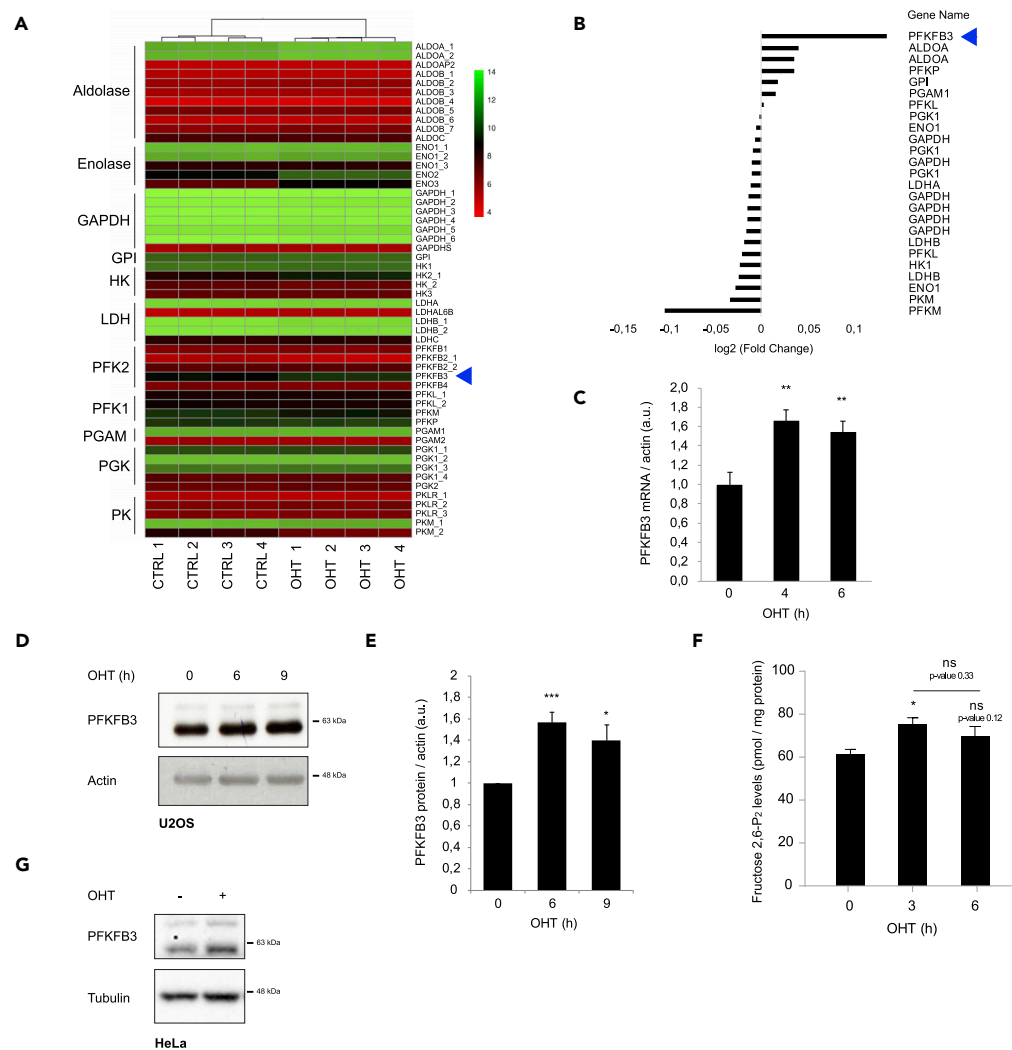
Figure 3. E2F1 Regulates PFKFB3 Expression

(A) Heatmap illustrating glycolytic genes expression in control (CTR) and E2F1-induced (OHT) U2OS cells upon 6 h OHT treatment from GEO: GSE39136 (Shats et al., 2013). The samples were clustered by column. Red-Green color scale indicates mRNA expression of each individual gene according to legend. Blue arrow indicates PFKFB3.

(B) Highly expressed glycolytic isoenzymes were plotted by Fold Change (FC) upon E2F1 induction. Cutoff of 1.05 FC was used to select up-regulated genes. Blue arrow indicates PFKFB3.

(C) U2OS ER-E2F1 cells were serum starved overnight, treated or not with OHT for 6 h. PFKFB3 mRNA levels were analyzed by quantitative RT-PCR. β-Actin was used to normalize gene expression.

(D) Cells were treated as described in (C), and PFKFB3 protein expression was analyzed by western blot at the indicated times. β-Actin was used as a loading control.

(E) Quantification of PFKFB3 expression was performed in n = 5 independent experiments and normalized by β-actin band intensities.

(F) Cells were treated as described in (C), and Fructose 2,6-P_2 levels were analyzed as described. Protein amount was used to normalize metabolite levels. Results show the measurement of n = 3 experiments.

(G) HeLa cells were transfected with ER-E2F1 plasmid, serum starved overnight, and treated or not with OHT for 6 h upon glucose starvation or rich conditions. PFKFB3 protein expression was analyzed by western blot at the indicated times. β-Actin was used as a loading control.

Data are presented as mean ± SD. Statistical significance is shown as: *p < 0.05; **p < 0.005; ***p < 0.001; ns: p > 0.05.

PFKFB3 activity on the translocation of mTORC1 to lysosomes (Figures 5C, 5D, and S5E). Altogether, these results demonstrate that PFKFB3 activity is required for E2F1-induced mTORC1 lysosomal translocation through Rag B.
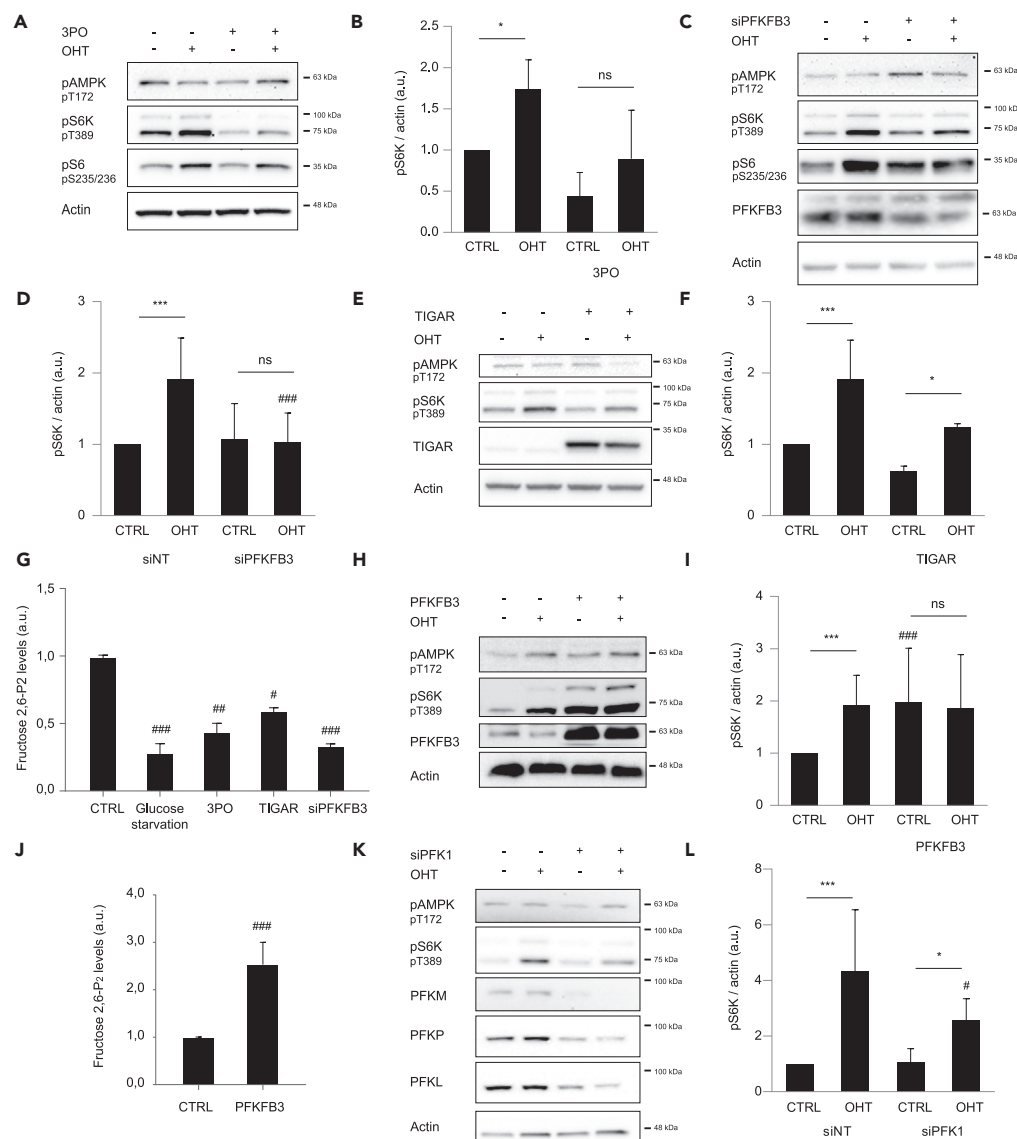
Figure 4. PFKFB3 Activity Regulates E2F1-Driven mTORC1 Activation

(A) U2OS ER-E2F1 cells were serum starved overnight, treated with (3-pyridinyl)-1-(4-pyridinyl)-2-propen-1-one (3PO) for 1 h before OHT treatment for 6 h. Indicated proteins were analyzed by western blot. β-Actin was used as a loading control.

(B) Intensity of S6K phosphorylation was analyzed in n = 3 independent experiments and normalized to β-actin band intensity.

(C) U2OS ER-E2F1 cells were transfected with small interfering RNA against PFKFB3 (siPFKFB3), serum starved overnight, and treated or not with OHT for 6 h. Indicated proteins were analyzed by western blot. β-Actin was used as a loading control.

(D) Intensity of S6K phosphorylation was analyzed in n = 3 independent experiments and normalized to β-actin band intensity.

(E) U2OS ER-E2F1 cells were transfected with empty vector (EV) or TIGAR expression plasmid, serum starved overnight, and treated or not with OHT for 6 h. Indicated proteins were analyzed by western blot. β-Actin was used as a loading control.

(F) Intensity of S6K phosphorylation was analyzed in n = 3 independent experiments and normalized to β-actin band intensity.

(G) Cells were treated as described, and Fructose 2,6-P$_2$ levels were analyzed. Protein amount was used to normalize metabolite levels. Results show the measurement of n = 3 independent experiments.

Figure 4. *Continued*

(H) U2OS ER-E2F1 cells were transfected with empty vector (EV) or PFKFB3 expression plasmid and serum starved overnight. OHT treatment for 6 h was performed. Indicated proteins were analyzed by western blot. β-Actin was used as a loading control.

(I) Intensity of S6K phosphorylation was analyzed in n = 3 independent experiments and normalized to β-actin band intensity.

(J) Cells were treated as described in (I), and Fructose 2,6-P$_2$ levels were analyzed. Protein amount was used to normalize metabolite levels. Results show the measurement of n = 3 independent experiments.

(K) U2OS ER-E2F1 cells were transfected with small interfering RNA against PFK1 isoenzymes PFK-M, PFK-L, and PFK-P (siPFK1); serum starved overnight; and treated or not with OHT for 6 h. Indicated proteins were analyzed by western blot. β-Actin was used as a loading control.

(L) Intensity of S6K phosphorylation was analyzed in n = 3 independent experiments and normalized to β-actin band intensity.

Data are presented as mean ± SD. Statistical significance is shown as: *p < 0.05; **p < 0.005; ***p < 0.001 for OHT effect compared with CTRL and #p < 0.05; ##p < 0.005; ###p < 0.001 for PFKFB3/PFK1 modulation compared with the respective control; ns: p > 0.05. See also Figure S4.

Despite an ample understanding about the biochemistry and regulation of the different glycolytic enzymes, their intracellular distribution remains unclear. We hypothesized that a glycolytic metabolon potentially containing phosphofructokinases enzymes might localize at the lysosome and mediate glucose sensing toward mTORC1. Thus, we assessed the presence of PFKFB3 and PFK1 enzymes at the lysosomes by FLAG-Rag B immunoprecipitation. Notably, both PFK1 and PFKFB3 pulled down with the mTORC1-regulatory protein Rag B (Figure 5E). Moreover, PFKFB3 binding was enhanced by the addition of OHT indicating that E2F1 potentiates PFKFB3 interaction, whereas PFK1 binding was not affected (Figures 5E–5G). Phosphofructokinases association with lysosomes was also supported by PFK1 and LAMP1 intracellular localization studies using Live-cell imaging in U2OS cells transiently expressing LAMP1-mRFP and PFKP-EGFP expression vectors (Webb et al., 2017). Although colocalization of both signals was barely detected, live imaging showed that PFKP-EGFP co-moved with LAMP1-mRFP-positive vesicles confirming a dynamic interaction between the metabolic enzyme PFK1 and the lysosomes (Figure 5H and Video S1). Altogether, these results indicate that phosphofructokinases axis regulates mTORC1 activity at the lysosomal surface potentially by a dynamic interaction with Rag B GTPase.

DISCUSSION

Many tumor cells rely on glucose metabolism not only for energy production, but also to promote cell proliferation and growth. In this work, we uncovered a novel function of lysosomes as a sensor platform of glucose catabolism in the regulation of mTORC1 activity by E2F1. We show that the increased glycolytic capacity conferred by E2F1 is linked to its ability to regulate mTORC1 activity. We identify the key glycolytic enzymes PFKFB3 and PFK1 as proteins associated with the lysosomal surface and demonstrate that the modulation of their activity, either by substrate accessibility or gene expression, regulates the translocation of mTORC1 to lysosomes and subsequently its activity. This study reveals a new function of phosphofructokinases axis as prominent regulators of mTORC1, parallel to their role on glycolysis. This regulation could represent an alternative mechanism for glucose sensing at the lysosomal surface.

We demonstrate that glucose potentiates E2F1-driven mTORC1 activation by an AMPK-independent pathway. It is widely established that growth and metabolic homeostasis are controlled by the coordination of mTORC1 and AMPK, as their activities are precisely regulated in opposite directions by glucose (Hardie, 2003). On the one hand, activation of AMPK by glucose deprivation inhibits mTORC1 by phosphorylating and consequently activating TSC2 or inhibiting RAPTOR (Gwinn et al., 2008; Inoki et al., 2006). On the other hand, under glucose starvation, the AMPK-associated proteins AXIN and LKB1 translocate to lysosomes where AMPK is localized and inhibit Ragulator GEF activity causing mTORC1 dissociation from lysosomes and consequent inactivation (Zhang et al., 2014). Accordingly, in the presence of glucose, mTORC1 was found highly localized in LAMP2-positive lysosomes, whereas AMPK was inactive. However, upon E2F1 induction, translocation of mTORC1 to lysosomes and mTORC1 activity were increased without detectable changes on AMPK activity both in glucose rich or starved conditions, suggesting the involvement of an AMPK-independent pathway. Interestingly, although glycolytic flux was enhanced, neither energetic rate nor AMPK phosphorylation was altered upon E2F1 induction, indicating that all the energy is redirected to anabolic cellular processes. In fact, protein synthesis, a process regulated by mTORC1, is the main energy consumer in cells. Our findings support the identification of a novel mechanism involving glucose control of mTORC1 activity in an AMPK-independent manner.
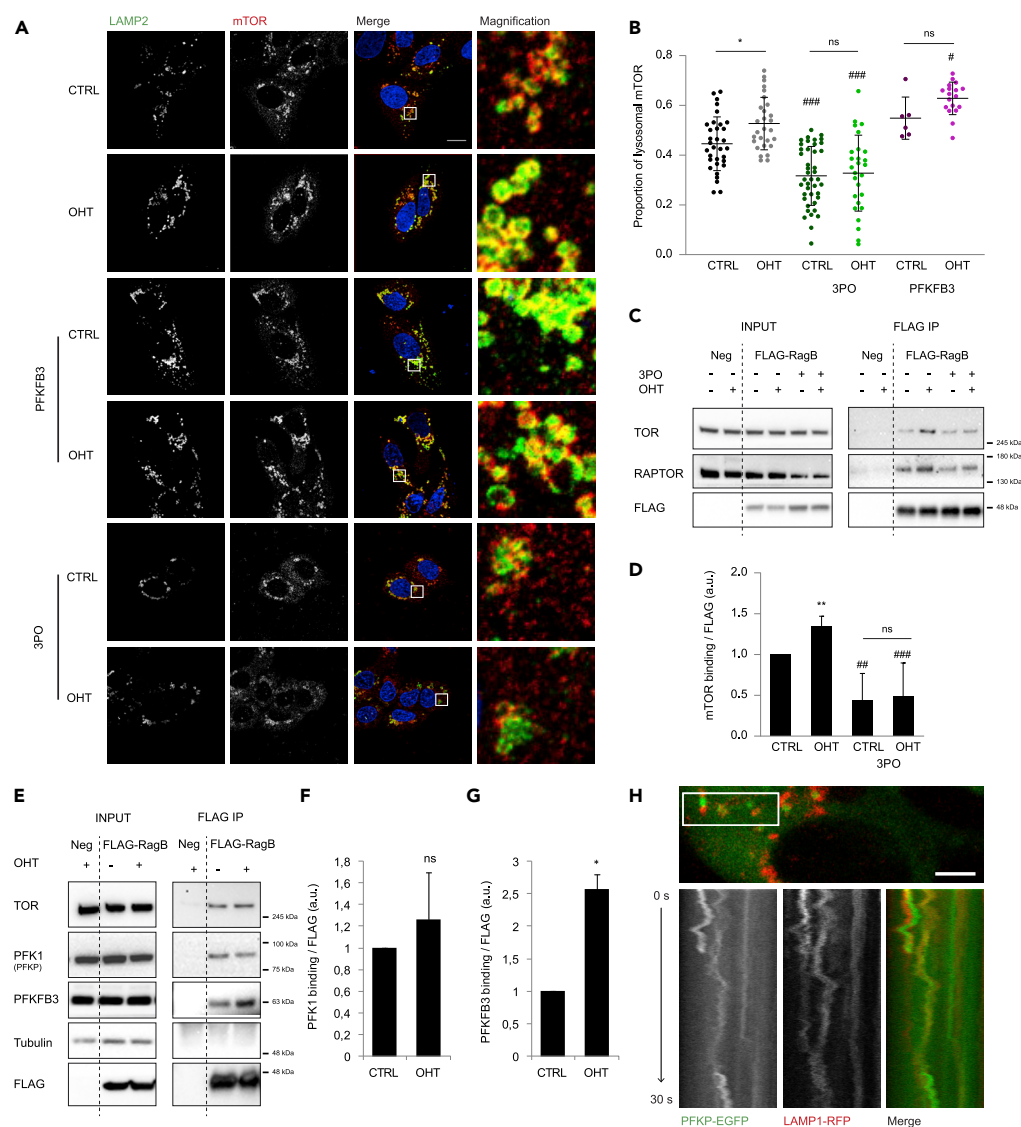
Figure 5. PFKFB3 Activity Modulates mTORC1 Recruitment Via Direct Interaction with Rag B

(A) U2OS ER-E2F1 cells were transfected as specified in Figure 4 and treated or not with OHT for 6 h mTOR (red) and LAMP2 (green) localization were analyzed by immunofluorescence. DAPI (blue) was used to stain the DNA. Scale bar corresponds to 10 μm.

(B) Quantification of lysosomal mTOR (red pixels co-localizing with green pixels compared with total red pixels).

(C) U2OS ER-E2F1 FLAG-Rag B cells were serum starved overnight and subjected to the indicated treatments for 1 h before OHT treatment for 6 h. FLAG-Rag B was immunoprecipitated and indicated proteins were analyzed by western blot. U2OS ER-E2F1 cells were used as a negative control for the immunoprecipitation.

(D) Quantification of mTOR band intensity normalized by FLAG was performed from n = 3 independent experiments.

(E) U2OS ER-E2F1 cells were serum starved overnight and treated with OHT for 6 h. FLAG-Rag B was immunoprecipitated, and indicated proteins were analyzed by western blot. U2OS ER-E2F1 cells were used as a negative control for the immunoprecipitation. Tubulin was used as a cytosolic protein control for unspecific binding.

(F and G) Quantification of PFKP (F) and PFKFB3 (G) band intensities normalized by FLAG was performed from n = 3 independent experiments.

(H) U2OS ER-E2F1 cells were transfected with plasmids encoding LAMP1-mCherry and PFKP-EGFP and analyzed by live-cell imaging. Kymograph analysis shows PFK1 moving together with LAMP1 vesicles along the trajectory shown in the upper panel. Scale bar corresponds to 5 μm.

Data are presented as mean ± SD. Statistical significance is shown as: *p < 0.05; **p < 0.005; ***p < 0.001 for OHT effect compared with CTRL and #p < 0.05; ##p < 0.005; ###p < 0.001 for PFKFB3 modulation compared with the respective control; ns: p > 0.05. See also Figure S5 and Video S1.

In addition to its role as a cell cycle regulator, E2F1 has been described as a master regulator of metabolism (Denechaud et al., 2017; Ouyang et al., 2009). By transcriptional regulation, E2F1 has been implicated in the switch from mitochondrial oxidative phosphorylation to aerobic glycolysis, a crucial metabolic alteration of many cancer cells (Blanchet et al., 2011). From our investigations, the PFK/FBPase isoform, PFKFB3, was identified as an E2F1-regulated gene whose expression and activity were essential for the regulation of mTORC1. PFK/FBPase is a well-known bifunctional enzyme that simultaneously catalyzes the formation and degradation of Fructose 2,6-P_2, the allosteric activator of PFK1, a rate-limiting enzyme that determines the glycolytic flux. Four PFK/FBPase isozymes have been described in humans (PFKFB1, PFKFB2, PFKFB3, and PFKFB4) that exert tissue-specific expression patterns and distinct kinase/phosphatase activity rates. Among them, PFKFB3 is the most frequently overexpressed in various human cancers and has been reported to promote proliferation and carcinogenesis (Yi et al., 2019). Indeed, the PFKFB3 isoform has the highest kinase/phosphatase activity rate (710:1), making it an extremely effective glycolysis inducer (Domenech et al., 2015; Manzano et al., 1999). Here, our results showing a correlation between PFKFB3 expression and Fructose 2,6-P_2 levels point out that transcriptional regulation is likely the predominant mechanism; however, we cannot exclude that other E2F1-induced signaling cascades could modulate PFKFB3 activity. In this regard, different protein kinases, such as RSK, MK2, PKA, Akt, PKC, and AMPK have been reported to phosphorylate and modulate PFKFB3 activity (Bartrons et al., 2018).

Key in this study is the demonstration that glycolysis is linked to mTORC1 pathway via the binding of PFKFB3 and PFK1 to the Rag B GTPase-Ragulator lysosomal scaffold. As far as we know, this is the first time that the key bifunctional enzyme PFKFB3 has been identified on lysosomes and, more importantly, has been associated with this non-glycolytic function. PFKFB3 activity promotes mTORC1 translocation to lysosomes and its consequent activation. It is well known that Fructose 2,6-P_2, the PFKFB3 product, is the major allosteric activator of PFK1 promoting the stabilization of the active PFK1 tetrameric form (Sola-Penna et al., 2010). We speculate that the PFK1 conformational change induced by Fructose 2,6-P_2 binding could be the responsible for mTOR recruitment to lysosomes. Supporting our hypothesis, previous reports identified PFK1 at the lysosomes and showed physical interaction with the ATP6V1a1 subunit of the v-ATPase (Su et al., 2003). Association of glycolytic enzymes to lysosomes has been suggested to represent a direct link between the v-ATPase and the glycolytic flux (Su et al., 2003). Based on this, we have drawn a model in which the presence of glucose, together with activation of glycolysis by E2F1-induced PFKFB3 expression, regulates mTORC1 activity.

From these results and others, lysosomes start to emerge as a scaffold platform for metabolic signaling pathways dictating the cell response to glucose scarcity. In addition of PFKFB3 and PFK1, other glycolytic enzymes have been reported to localize at lysosomes such as lactate dehydrogenase, GAPDH, and Aldolase (Brisson et al., 2016; Lee et al., 2009; Zhang et al., 2017). Interestingly, Fructose 1,6-P_2 levels, the PFK1 catalytic product and Aldolase subtract, has been identified as an essential mediator of glucose sensing by AMPK through Ragulator complex modulation (Zhang et al., 2017). Thus, the ability of the lysosome to integrate the nutritional status of the cell turns it into a perfect candidate for the modulation of master regulators of cell anabolism and catabolism such as AMPK or mTORC1.

Parallel to the role of lysosomes as metabolic hubs, their peripheral distribution has been correlated with invasion and metastasis, one of the hallmarks of cancer. Dramatic changes in lysosomal volume, composition, and localization have been reported during transformation and cancer progression (Appelqvist et al., 2013). Localization of lysosomes shifts from a perinuclear to a peripheral pattern in cancer cells, particularly those at the invasive edges of tumors, suggesting an increased lysosomal exocytosis (Kroemer and Jaattela, 2005). Lysosomes undergo exocytosis in most cell types; however, in tumor cells this process is highly activated, which promotes extracellular acidification, facilitating extracellular matrix degradation and stimulating angiogenesis, tumor growth, and invasion (Appelqvist et al., 2013; Machado et al., 2015). Previous results from our laboratory demonstrate that E2F1 regulates lysosomal function by altering both lysosomal activity and intracellular localization (Meo-Evoli et al., 2015). Here, we show that glucose is also necessary for shifting lysosomes from a perinuclear to a peripheral localization, pointing out the integrative function of this organelle coordinating glucose catabolism and cell growth. In fact, the PFK1 isoform P that we detected associated with Rag B GTPase has also been identified interacting with the BLOC-one-related complex (BORC), a multisubunit complex that mediates lysosome anterograde trafficking (Pu et al., 2015), supporting the notion that PFK1 is effectively associated with lysosomes.

Conclusively, we believe that identifying PFKFB3 and PFK1 as a part of the complex associated with Rag B GTPase-Ragulator lysosomal scaffold lays the ground for understanding how glucose regulates mTORC1 independently of AMPK.

Limitations of the Study

Our results identified PFK1 as a part of the complex associated with the RagB GTPase-Ragulator lysosomal scaffold, which conditionally interacts with PFKFB3 enzyme. This finding supports the notion of the lysosome as a metabolic hub for glucose sensing toward mTORC1; however, the precise mechanism by which the phosphofructokinases regulate mTORC1 remains unresolved. Recent reports demonstrate that AMPK is localized on the lysosomal surface and regulated by aldolase (Zhang et al., 2017). However, the interconnection between mTORC1/phosphofructokinases and AMPK/aldolase still remains unclear. Finally, Ragulator being a main player coupling amino acid signaling to both lysosomal positioning and mTORC1, our data on the impact of glucose on both processes might suggest a common molecular machinery controlling nutrient sensing (Pu et al., 2017; Zoncu et al., 2011). Nevertheless, further investigations will be required to characterize the detailed mechanism of glucose sensing at the lysosome.

METHODS

All methods can be found in the accompanying Transparent Methods supplemental file.

SUPPLEMENTAL INFORMATION

Supplemental Information can be found online at https://doi.org/10.1016/j.isci.2019.09.040.

AUTHOR CONTRIBUTIONS

E.A. designed and performed most of the experiments. A.M. achieved Fructose 2,6-P_2 levels analysis. E.A., J.P., and C.M. performed the experiments required for the revision. E.A., J.P., A.G., S.A., C.M., and A.T. analyzed and discussed the data. E.A. and A.T. wrote the manuscript. A.T. conceived the study. A.T. and C.M. coordinated the study. All authors intellectually contributed and commented on the manuscript.

DECLARATION OF INTERESTS

The authors declare no competing interests.

REFERENCES

Agger, K., Santoni-Rugiu, E., Holmberg, C., Karlstrom, O., and Helin, K. (2005). Conditional E2F1 activation in transgenic mice causes testicular atrophy and dysplasia mimicking human CIS. Oncogene 24, 780–789.

Appelqvist, H., Waster, P., Kagedal, K., and Ollinger, K. (2013). The lysosome: from waste bag to potential therapeutic target. J. Mol. Cell Biol. 5, 214–226.

Bar-Peled, L., Schweitzer, L.D., Zoncu, R., and Sabatini, D.M. (2012). Ragulator is a GEF for the rag GTPases that signal amino acid levels to mTORC1. Cell 150, 1196–1208.

Bartrons, R., Simon-Molas, H., Rodriguez-Garcia, A., Castano, E., Navarro-Sabate, A., Manzano, A., and Martinez-Outschoorn, U.E. (2018). Fructose 2,6-bisphosphate in cancer cell metabolism. Front. Oncol. 8, 331.

Bensaad, K., Tsuruta, A., Selak, M.A., Vidal, M.N., Nakano, K., Bartrons, R., Gottlieb, E., and Vousden, K.H. (2006). TIGAR, a p53-inducible regulator of glycolysis and apoptosis. Cell 126, 107–120.

Bieda, M., Xu, X., Singer, M.A., Green, R., and Farnham, P.J. (2006). Unbiased location analysis of E2F1-binding sites suggests a widespread role for E2F1 in the human genome. Genome Res. 16, 595–605.

Blanchet, E., Annicotte, J.S., Lagarrigue, S., Aguilar, V., Clape, C., Chavey, C., Fritz, V., Casas, F., Apparailly, F., Auwerx, J., et al. (2011). E2F transcription factor-1 regulates oxidative metabolism. Nat. Cell Biol. 13, 1146–1152.

Brisson, L., Banski, P., Sboarina, M., Dethier, C., Danhier, P., Fontenille, M.J., Van Hee, V.F., Vazeille, T., Tardy, M., Falces, J., et al. (2016). Lactate dehydrogenase B controls lysosome activity and autophagy in cancer. Cancer Cell 30, 418–431.

Clem, B., Telang, S., Clem, A., Yalcin, A., Meier, J., Simmons, A., Rasku, M.A., Arumugam, S., Dean, W.L., Eaton, J., et al. (2008). Small-molecule inhibition of 6-phosphofructo-2-kinase activity suppresses glycolytic flux and tumor growth. Mol. Cancer Ther. 7, 110–120.

Denechaud, P.D., Fajas, L., and Giralt, A. (2017). E2F1, a novel regulator of metabolism. Front. Endocrinol. (Lausanne) 8, 311.

Domenech, E., Maestre, C., Esteban-Martinez, L., Partida, D., Pascual, R., Fernandez-Miranda, G., Seco, E., Campos-Olivas, R., Perez, M., Megias, D., et al. (2015). AMPK and PFKFB3 mediate glycolysis and survival in response to mitophagy during mitotic arrest. Nat. Cell Biol. 17, 1304–1316.

Darville, M.I., Antoine, I.V., Mertens-Strilthagen, J.R., Dupriez, V.J., and Rousseau, G.G. (1995). An E2F-dependent late-serum-response promoter in a gene that controls glycolysis. Oncogene 11, 1509–1517.

Duran, J., Navarro-Sabate, A., Pujol, A., Perales, J.C., Manzano, A., Obach, M., Gomez, M., and Bartrons, R. (2008). Overexpression of ubiquitous 6-phosphofructo-2-kinase in the liver of

transgenic mice results in weight gain. Biochem. Biophys. Res. Commun. 365, 291–297.

Eymin, B., Gazzeri, S., Brambilla, C., and Brambilla, E. (2001). Distinct pattern of E2F1 expression in human lung tumours: E2F1 is upregulated in small cell lung carcinoma. Oncogene 20, 1678–1687.

Gordan, J.D., Thompson, C.B., and Simon, M.C. (2007). HIF and c-Myc: sibling rivals for control of cancer cell metabolism and proliferation. Cancer Cell 12, 108–113.

Gwinn, D.M., Shackelford, D.B., Egan, D.F., Mihaylova, M.M., Mery, A., Vasquez, D.S., Turk, B.E., and Shaw, R.J. (2008). AMPK phosphorylation of raptor mediates a metabolic checkpoint. Mol. Cell 30, 214–226.

Hardie, D.G. (2003). Minireview: the AMP-activated protein kinase cascade: the key sensor of cellular energy status. Endocrinology 144, 5179–5183.

Inoki, K., Li, Y., Zhu, T., Wu, J., and Guan, K.L. (2002). TSC2 is phosphorylated and inhibited by Akt and suppresses mTOR signalling. Nat. Cell Biol. 4, 648–657.

Inoki, K., Ouyang, H., Zhu, T., Lindvall, C., Wang, Y., Zhang, X., Yang, Q., Bennett, C., Harada, Y., Stankunas, K., et al. (2006). TSC2 integrates Wnt and energy signals via a coordinated phosphorylation by AMPK and GSK3 to regulate cell growth. Cell 126, 955–968.

Kim, E., Goraksha-Hicks, P., Li, L., Neufeld, T.P., and Guan, K.L. (2008). Regulation of TORC1 by Rag GTPases in nutrient response. Nat. Cell Biol. 10, 935–945.

Korolchuk, V.I., Saiki, S., Lichtenberg, M., Siddiqi, F.H., Roberts, E.A., Imarisio, S., Jahreiss, L., Sarkar, S., Futter, M., Menzies, F.M., et al. (2011). Lysosomal positioning coordinates cellular nutrient responses. Nat. Cell Biol. 13, 453–460.

Kroemer, G., and Jaattela, M. (2005). Lysosomes and autophagy in cell death control. Nature reviews. Cancer 5, 886–897.

Ladu, S., Calvisi, D.F., Conner, E.A., Farina, M., Factor, V.M., and Thorgeirsson, S.S. (2008). E2F1 inhibits c-Myc-driven apoptosis via PIK3CA/Akt/mTOR and COX-2 in a mouse model of human liver cancer. Gastroenterology 135, 1322–1332.

Lee, M.N., Ha, S.H., Kim, J., Koh, A., Lee, C.S., Kim, J.H., Jeon, H., Kim, D.H., Suh, P.G., and Ryu, S.H. (2009). Glycolytic flux signals to mTOR through glyceraldehyde-3-phosphate dehydrogenase-mediated regulation of Rheb. Mol. Cell Biol. 29, 3991–4001.

Ma, L., Chen, Z., Erdjument-Bromage, H., Tempst, P., and Pandolfi, P.P. (2005). Phosphorylation and functional inactivation of TSC2 by Erk implications for tuberous sclerosis and cancer pathogenesis. Cell 121, 179–193.

Machado, E., White-Gilbertson, S., van de Vlekkert, D., Janke, L., Moshiach, S., Campos, Y., Finkelstein, D., Gomero, E., Mosca, R., Qiu, X., et al. (2015). Regulated lysosomal exocytosis mediates cancer progression. Sci. Adv. 1, e1500603.

Manning, B.D., and Cantley, L.C. (2007). AKT/PKB signaling: navigating downstream. Cell 129, 1261–1274.

Manzano, A., Perez, J.X., Nadal, M., Estivill, X., Lange, A., and Bartrons, R. (1999). Cloning, expression and chromosomal localization of a human testis 6-phosphofructo-2-kinase/fructose-2,6-bisphosphatase gene. Gene 229, 83–89.

Menon, S., and Manning, B.D. (2008). Common corruption of the mTOR signaling network in human tumors. Oncogene 27 (Suppl 2), S43–S51.

Meo-Evoli, N., Almacellas, E., Massucci, F.A., Gentilella, A., Ambrosio, S., Kozma, S.C., Thomas, G., and Tauler, A. (2015). V-ATPase: a master effector of E2F1-mediated lysosomal trafficking, mTORC1 activation and autophagy. Oncotarget 6, 28057–28070.

Molina-Privado, I., Rodriguez-Martinez, M., Rebollo, P., Martin-Perez, D., Artiga, M.J., Menarguez, J., Flemington, E.K., Piris, M.A., and Campanero, M.R. (2009). E2F1 expression is deregulated and plays an oncogenic role in sporadic Burkitt's lymphoma. Cancer Res. 69, 4052–4058.

Moon, J.S., Hisata, S., Park, M.A., DeNicola, G.M., Ryter, S.W., Nakahira, K., and Choi, A.M.K. (2015). mTORC1-Induced HK1-dependent glycolysis regulates NLRP3 inflammasome activation. Cell Rep. 12, 102–115.

Oki, S., Limnander, A., Yao, P.M., Niki, M., Pandolfi, P.P., and Rothman, P.B. (2005). Dok1 and SHIP act as negative regulators of v-Abl-induced pre-B cell transformation, proliferation and Ras/Erk activation. Cell Cycle 4, 310–314.

Ouyang, Z., Zhou, Q., and Wong, W.H. (2009). ChIP-Seq of transcription factors predicts absolute and differential gene expression in embryonic stem cells. Proc. Natl. Acad. Sci. U S A 106, 21521–21526.

Pavlova, N.N., and Thompson, C.B. (2016). The emerging hallmarks of cancer metabolism. Cell Metab. 23, 27–47.

Pilkis, S.J., El-Maghrabi, M.R., Pilkis, J., Claus, T.H., and Cumming, D.A. (1981). Fructose 2,6-bisphosphate. A new activator of phosphofructokinase. J. Biol. Chem. 256, 3171–3174.

Pourdehnad, M., Truitt, M.L., Siddiqi, I.N., Ducker, G.S., Shokat, K.M., and Ruggero, D. (2013). Myc and mTOR converge on a common node in protein synthesis control that confers synthetic lethality in Myc-driven cancers. Proc. Natl. Acad. Sci. U S A 110, 11988–11993.

Pu, J., Keren-Kaplan, T., and Bonifacino, J.S. (2017). A Ragulator–BORC interaction controls lysosome positioning in response to amino acid availability. J. Cell Biol. https://doi.org/10.1083/jcb.201703094.

Pu, J., Schindler, C., Jia, R., Jarnik, M., Backlund, P., and Bonifacino, J.S. (2015). BORC, a multisubunit complex that regulates lysosome positioning. Dev. Cell 33, 176–188.

Ramanathan, A., Wang, C., and Schreiber, S.L. (2005). Perturbational profiling of a cell-line

model of tumorigenesis by using metabolic measurements. Proc. Natl. Acad. Sci. U S A *102*, 5992–5997.

Real, S., Meo-Evoli, N., Espada, L., and Tauler, A. (2011). E2F1 regulates cellular growth by mTORC1 signaling. PLoS One *6*, e16163.

Sancak, Y., Bar-Peled, L., Zoncu, R., Markhard, A.L., Nada, S., and Sabatini, D.M. (2010). Ragulator-Rag complex targets mTORC1 to the lysosomal surface and is necessary for its activation by amino acids. Cell *141*, 290–303.

Saxton, R.A., and Sabatini, D.M. (2017). mTOR signaling in growth, metabolism, and disease. Cell *169*, 361–371.

Shats, I., Gatza, M.L., Liu, B., Angus, S.P., You, L., and Nevins, J.R. (2013). FOXO transcription factors control E2F1 transcriptional specificity and apoptotic function. Cancer Res. *73*, 6056–6067.

Sola-Penna, M., Da Silva, D., Coelho, W.S., Marinho-Carvalho, M.M., and Zancan, P. (2010). Regulation of mammalian muscle type 6-phosphofructo-1-kinase and its implication for the control of the metabolism. IUBMB Life *62*, 791–796.

Su, Y., Zhou, A., Al-Lamki, R.S., and Karet, F.E. (2003). The a-subunit of the V-type H+-ATPase interacts with phosphofructokinase-1 in humans. J. Biol. Chem. *278*, 20013–20018.

Tarangelo, A., Lo, N., Teng, R., Kim, E., Le, L., Watson, D., Furth, E.E., Raman, P., Ehmer, U., and Viatour, P. (2015). Recruitment of Pontin/Reptin by E2f1 amplifies E2f transcriptional response during cancer progression. Nat. Commun. *6*, 10028.

Thomas, H.E., Mercer, C.A., Carnevalli, L.S., Park, J., Andersen, J.B., Conner, E.A., Tanaka, K., Matsutani, T., Iwanami, A., Aronow, B.J., et al. (2012). mTOR inhibitors synergize on regression, reversal of gene expression, and autophagy in hepatocellular carcinoma. Sci. Transl. Med. *4*, 139ra184.

Van Schaftingen, E., Lederer, B., Bartrons, R., and Hers, H.G. (1982). A kinetic study of pyrophosphate: fructose-6-phosphate phosphotransferase from potato tubers. Application to a microassay of fructose 2,6-bisphosphate. Eur. J. Biochem. *129*, 191–195.

Wang, L.Y., Hung, C.L., Chen, Y.R., Yang, J.C., Wang, J., Campbell, M., Izumiya, Y., Chen, H.W., Wang, W.C., Ann, D.K., et al. (2016). KDM4A coactivates E2F1 to regulate the PDK-dependent metabolic switch between mitochondrial oxidation and glycolysis. Cell Rep. *16*, 3016–3027.

Warburg, O. (1956). On the origin of cancer cells. Science *123*, 309–314.

Webb, B.A., Dosey, A.M., Wittmann, T., Kollman, J.M., and Barber, D.L. (2017). The glycolytic enzyme phosphofructokinase-1 assembles into filaments. J. Cell Biol. *216*, 2305–2313.

Wolfson, R.L., and Sabatini, D.M. (2017). The dawn of the age of amino acid sensors for the mTORC1 pathway. Cell Metab. *26*, 301–309.

Wu, M., Seto, E., and Zhang, J. (2015). E2F1 enhances glycolysis through suppressing Sirt6 transcription in cancer cells. Oncotarget *6*, 11252–11263.

Zhang, S.Y., Liu, S.C., Al-Saleem, L.F., Holloran, D., Babb, J., Guo, X., and Klein-Szanto, A.J. (2000). E2F-1: a proliferative marker of breast neoplasia. Cancer Epidemiol. Biomarkers Prev. *9*, 395–401.

Zhang, C.-S., Jiang, B., Li, M., Zhu, M., Peng, Y., Zhang, Y.-L., Wu, Y.-Q., Li, T.Y., Liang, Y., Lu, Z., et al. (2014). The lysosomal v-ATPase-Ragulator complex is a common activator for AMPK and mTORC1, acting as a switch between catabolism and anabolism. Cell Metab. *20*, 526–540.

Yi, M., Ban, Y., Tan, Y., Xiong, W., Li, G., and Xiang, B. (2019). 6-Phosphofructo-2-kinase/fructose-2,6-biphosphatase 3 and 4: a pair of valves for fine-tuning of glucose metabolism in human cancer. Mol Metab. *20*, 1–13.

Zhang, C.S., Hawley, S.A., Zong, Y., Li, M., Wang, Z., Gray, A., Ma, T., Cui, J., Feng, J.W., Zhu, M., et al. (2017). Fructose-1,6-bisphosphate and aldolase mediate glucose sensing by AMPK. Nature *548*, 112–116.

Zoncu, R., Bar-Peled, L., Efeyan, A., Wang, S., Sancak, Y., and Sabatini, D.M. (2011). mTORC1 senses lysosomal amino acids through an inside-out mechanism that requires the vacuolar H(+)-ATPase. Science *334*, 678–683.

Supplemental Information

Phosphofructokinases Axis Controls

Glucose-Dependent mTORC1 Activation

Driven by E2F1

Eugènia Almacellas, Joffrey Pelletier, Anna Manzano, Antonio Gentilella, Santiago Ambrosio, Caroline Mauvezin, and Albert Tauler

SUPPLEMENTAL FIGURES AND LEGENDS

A

B

C

HeLa

D

E

F

G

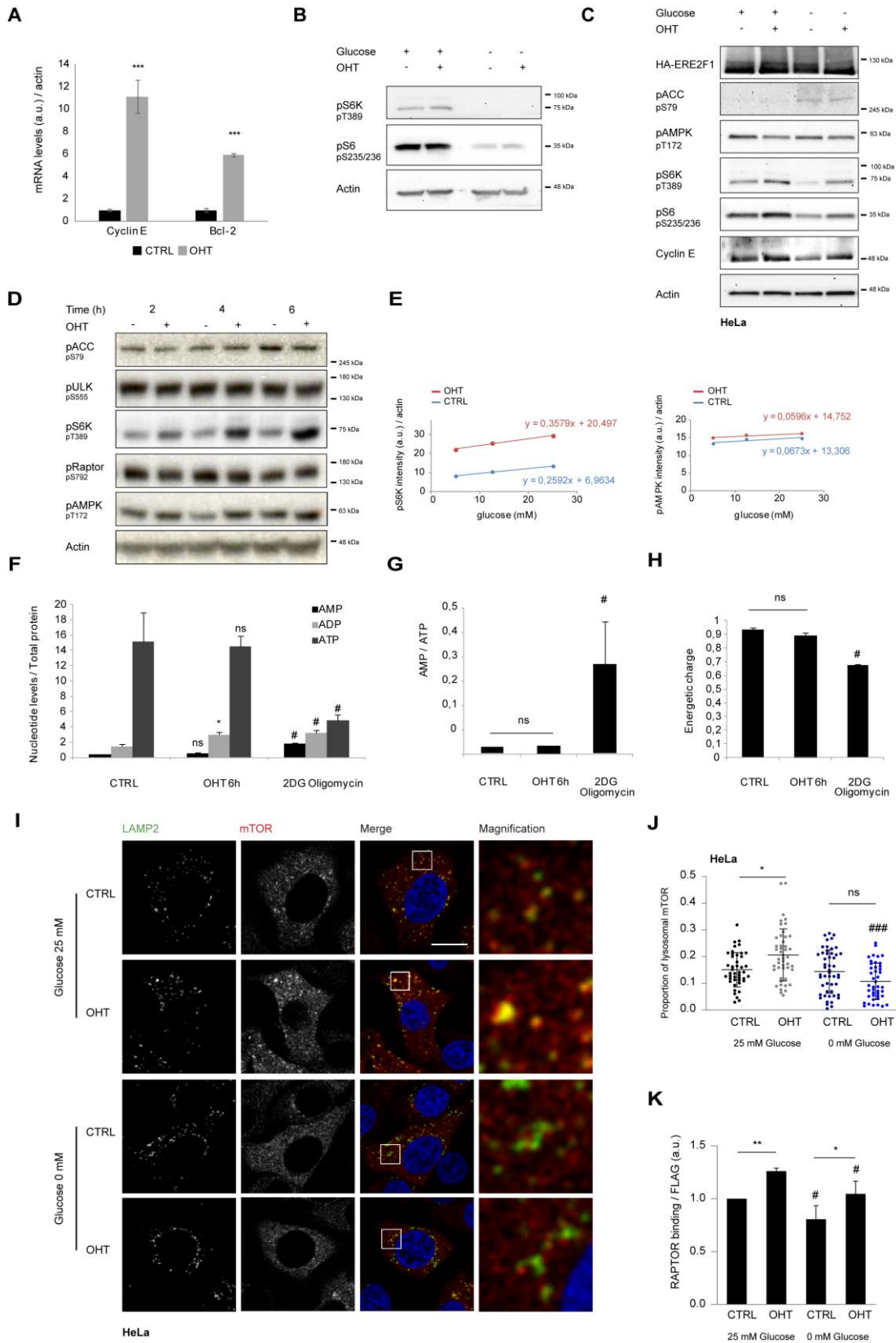**H**

I

HeLa

J

HeLa

K

Figure S1. E2F1 does not affect cellular energetic balance. Related to Figure 1. (A) U2OS ER-E2F1 cells were serum starved over-night and treated or not with OHT for 6 hours. mRNA levels of indicated genes were analyzed by quantitative PCR and normalized by β-actin. (B) U2OS cells were serum starved over-night, glucose starved for one hour prior to OHT treatment for 6 hours. Indicated proteins were analyzed by Western Blot. β-actin was used as a loading control. (C) HeLa cells transiently expressing ER-E2F1 plasmid were serum starved over-night, cultured in presence (25 mM) or absence (0 mM) of glucose for one hour prior to OHT treatment for 6 hours. Indicated proteins were analyzed by Western Blot. β-actin was used as a loading control. (D) U2OS ER-E2F1 cells were serum starved over-night and treated with OHT for different times. Indicated proteins were analyzed by Western Blot. β-actin was used as a loading control. (E) Band intensities of pS6K and pAMPK of Figure 1C were normalized to β-actin and plotted. Linear regression is shown. (F-H) U2OS ER-E2F1 cells were serum starved over-night and treated with OHT for 6 hours or 2DG + Oligomycin A. Samples were subjected to UPLC and data was normalized to protein concentration (F), AMP/ATP ratio (G) and energy charge ([ATP]+1/2 [ADP])/([ATP]+[ADP]+[AMP]) (H) were calculated. (I) HeLa cells transiently expressing ERE2F1 were treated as described in panel C. mTOR (red) and LAMP2 (green) were identified by Immunofluorescence analysis under indicated experimental conditions. DAPI (blue) was used to stain the nucleus. Scale bar corresponds to 10 μm. (J) Quantification of lysosomal mTOR (red pixels co-localizing with green pixels compared to total red pixels). (K) Band intensities of Raptor normalized by FLAG intensity from Figure 1F was measured and plotted in n = 3 independent immunoprecipitation experiments. Data are presented as mean ± SD. Statistical significance is shown as: *$p < 0.05$; **$p < 0.005$; ***$p < 0.001$ for OHT effect compared to CTRL and # $p < 0.05$; ## $p < 0.005$; ## $p < 0.001$ for indicated condition compared to the respective control; ns: $p > 0.05$.
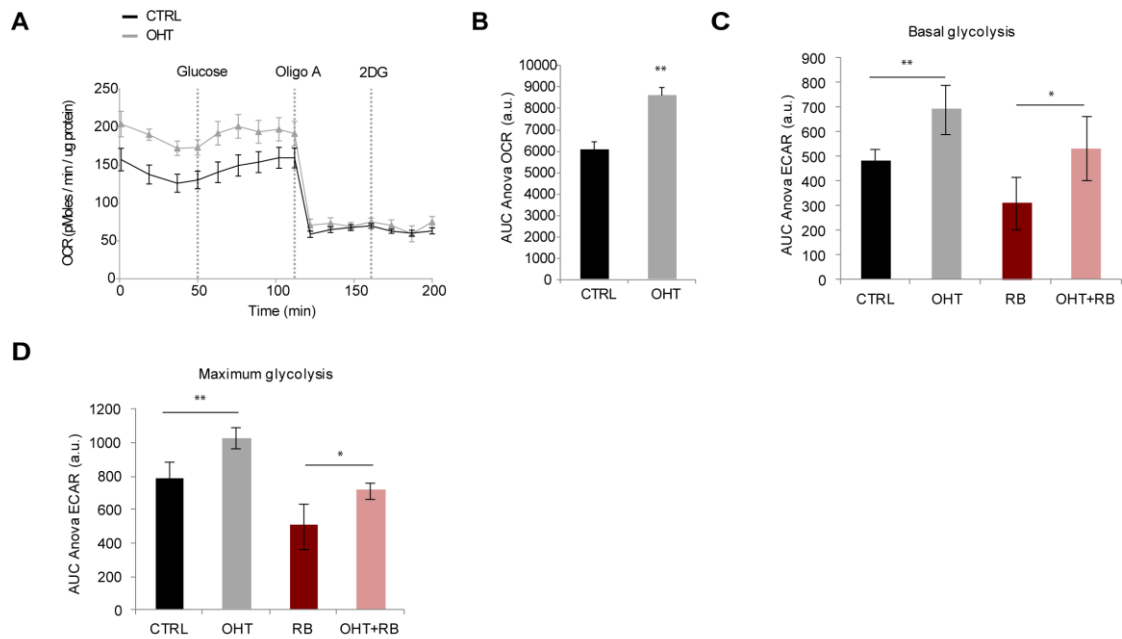
Figure S2. Oxygen Consumption on E2F1-induced cells. Related to Figure 2. (A) Representative OCR of GlycoStress Test result performed in U2OS ER-E2F1 cells pre-treated with OHT for 6 hours and subjected to SeaHorse analysis. n = 3 independent experiments showed similar results. (B) Area Under the Curve (AUC) analysis of measurements 1-9 indicating Oxygen Consumption upon E2F1 induction. (C) Area Under the Curve (AUC) analysis of measurements from glucose injection to Oligo A indicating basal glycolysis. (D) Area Under the Curve (AUC) analysis of measurements Oligo A and 2DG indicating maximum glycolysis. Data are presented as mean ± SD. Statistical significance is shown as: *p < 0.05; **p < 0.005; ***p < 0.001; ns: p > 0.05.
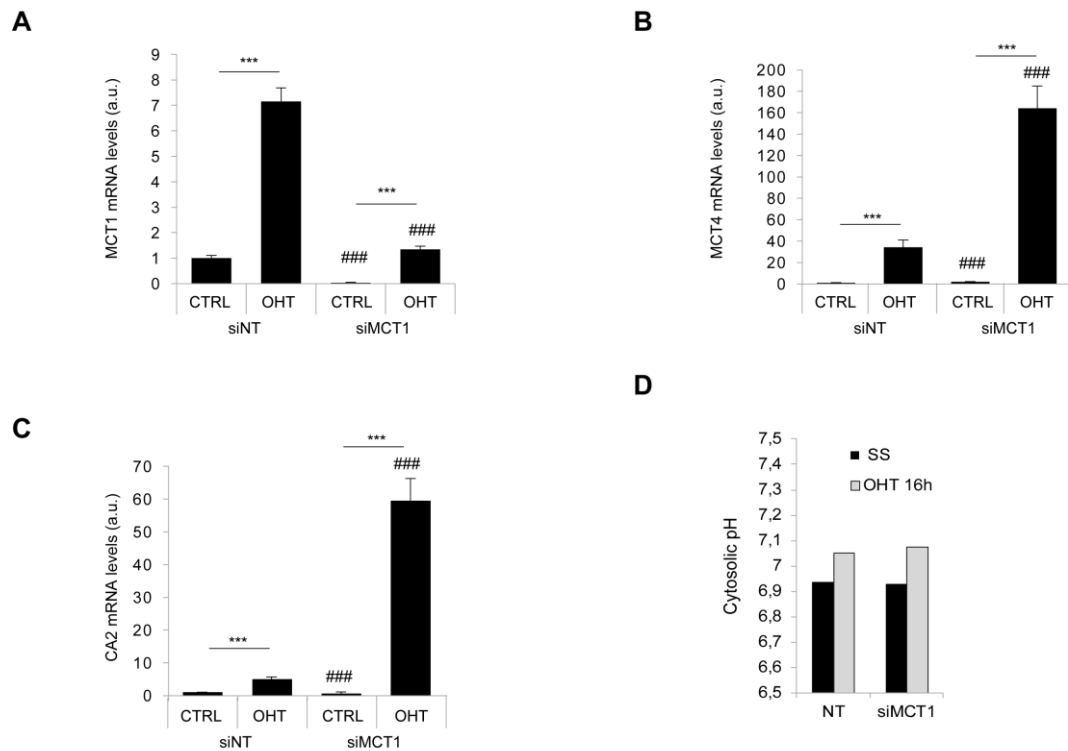
Figure S3. E2F1 regulates the expression of proton transporters and carbonic anhydrase 2. Related to Figure 2. (A-C) U2OS ER-E2F1 cells were transfected with small interfering RNA control (siNT) or MCT1 (siMCT1). Then, cells were serum starved over-night and treated with OHT for 6 hours. RNA levels of MCT1 (A), MCT4 (B) or CA2 (C) were analyzed by quantitative PCR and normalized by β-actin. (D) U2OS ER-E2F1 cells were transfected with small interfering RNA control (siNT) or MCT1 (siMCT1). Then, cells were serum starved over-night and treated with OHT for 16 hours. SNARF-AM ester was used to determine cytosolic pH based on standard curve with adjusted pH. Data are presented as mean ± SD. Statistical significance is shown as: *$p < 0.05$; **$p < 0.005$; ***$p < 0.001$ for OHT effect compared to CTRL and # $p < 0.05$; ## $p < 0.005$; ## $p < 0.001$ for indicated condition compared to the respective control; ns: $p > 0.05$.
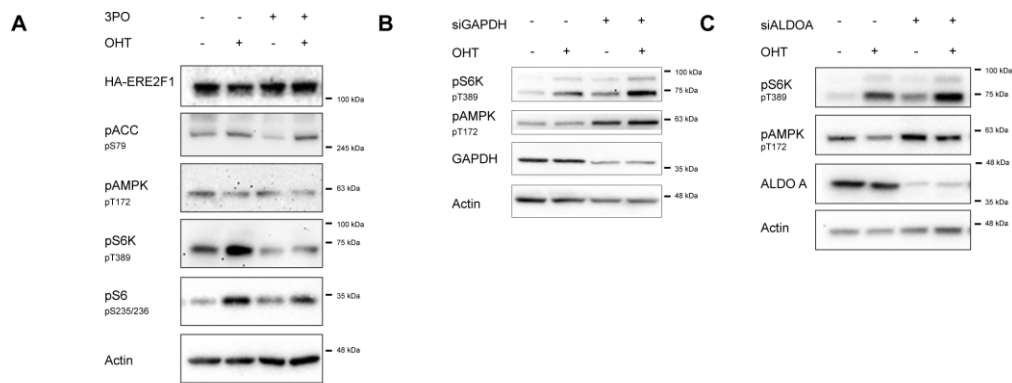
Figure S4. Effect of Aldolase and GAPDH depletion on mTORC1. Related to Figure 4. (A) HeLa cells transiently expressing ER-E2F1 plasmid were serum starved over-night and treated or not with 3PO for one hour prior to OHT treatment for 6 hours. Indicated proteins were analyzed by Western Blot. β-actin was used as a loading control. (B-C) U2OS ER-E2F1 cells were transfected with small interfering RNA against GAPDH (siGAPDH) (B) or Aldolase A (siALDO A) (C), serum starved over-night and treated or not with OHT for 6 hours. Indicated proteins were analyzed by Western Blot. β-actin was used as a loading control. Statistical significance is shown as: *p < 0.05; **p < 0.005; ***p < 0.001; ns: p > 0.05.
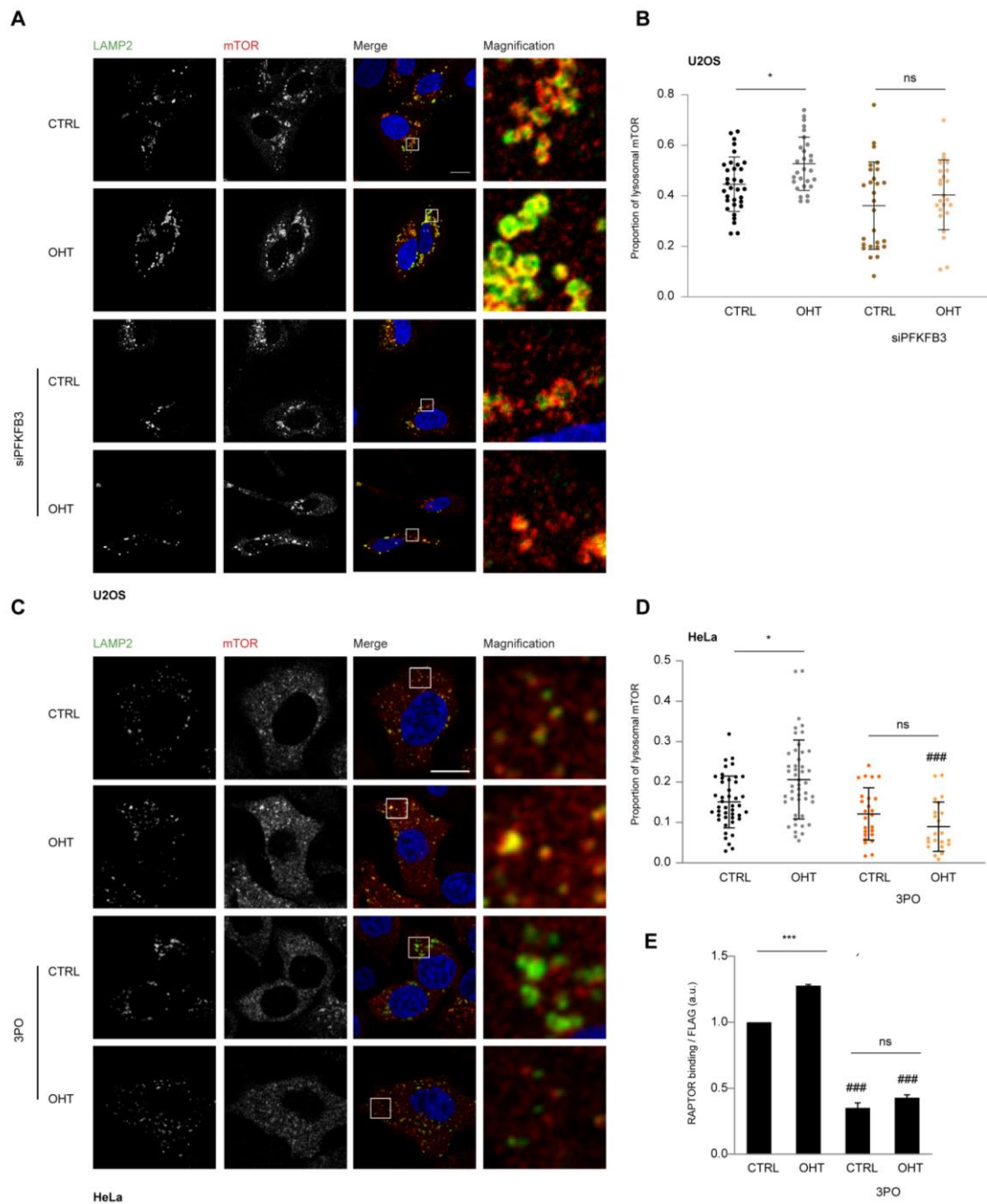
Figure S5. PFKFB3 depletion reduces mTORC1 lysosomal recruitment. Related to

Figure 5. (A) U2OS ER-E2F1 cells were transfected with small interfering RNA against

PFKFB3 and treated or not with OHT for 6 hours. Immunofluorescence of mTOR (red)

and LAMP2 (green) was performed. DAPI (blue) was used to stain the nucleus. Scale

bar corresponds to 10 μm. (B) Quantification of lysosomal mTOR (red pixels co-localizing

with green pixels compared to total red pixels). (C) HeLa cells transiently expressing ER-

E2F1 plasmid were serum starved over-night and treated or not with 3PO for one hour prior to OHT treatment for 6 hours. mTOR (red) and LAMP2 (green) were identified by Immunofluorescence analysis under indicated experimental conditions. DAPI (blue) was used to stain the nucleus. Scale bar corresponds to 10 μm. (D) Quantification of lysosomal mTOR (red pixels co-localizing with green pixels compared to total red pixels). (E) Quantification of Raptor band intensity normalized by FLAG was performed from n = 3 independent experiments. Data are presented as mean ± SD. Statistical significance is shown as: *$p < 0.05$; **$p < 0.005$; ***$p < 0.001$ for OHT effect compared to CTRL and # $p < 0.05$; ## $p < 0.005$; ## $p < 0.001$ for indicated condition compared to the respective control; ns: $p > 0.05$.

SUPPLEMENTAL TABLES

Gene	Sequence [dT][dT] (5' - 3')	[siRNA]	Brand
ALDO A	CCAACAGCCUUGCCUGUCAAGGAAA	20 nM	Sigma
GAPDH	CGGGAAGCUCACUGGCAUG	50 nM	Sigma
PFKFB3	GCUGUGAAGCAGUACAGCUCCUAC	20 nM	Sigma
PFKL	CGAGAACAACUGGAACAUUUA	20 nM	Sigma
PFKM	CCUCCAGAAAGCAGGUAAGAUC	20 nM	Sigma
PFKP	AGGAACGGCCAGAUCGAUA	20 nM	Sigma

Table S1. Related to Figures 4, S4 and Transparent methods. List of small interfering

RNA (siRNA) used in this study.

Primary antibodies			
Antigen	Dilution	Source	Catalog Number
ß-actin	1/10000	Sigma	A2228
ALDO A	1/1000	Abcam	ab169544
Cyclin E	1/1000	Cell signaling Tech	4129
FLAG	1/2000	Sigma	F7425
GAPDH	1/1000	Cell signaling Tech	2118
HA	1/5000	Roche	11583816001
mTOR	1/1000	Cell Signaling Tech	2983
pACC S79	1/1000	Cell Signaling Tech	3661S
pAMPK T172	1/1000	Cell Signaling Tech	2535S
PFKFB3	1/2000	Proteintech	13763-1-AP
PFKL	1/1000	NOVUS	NBP1-56607
PFKM	1/1000	Abcam	ab154804
PFKP	1/1000	Cell Signaling Tech	12764
pRaptor S792	1/1000	Cell Signaling Tech	2083
pS6 S235/236	1/1000	Cell Signaling Tech	2211
pS6K T389	1/1000	Cell signaling Tech	9206
pULK S555	1/1000	Cell Signaling Tech	5869
Raptor	1/1000	Millipore	09-217
TIGAR (M-209)	1/1000	Santa Cruz Biotech	sc-67273
α-tubulin	1/1000	Sigma	T6074
Secondary antibodies			
Antigen	Dilution	Source	Catalog Number
Anti-Mouse Ig HRP	1/5000	Dako	P0260
Anti-Rabbit Ig HRP	1/5000	Dako	P0399

Table S2. Related to Figures 1-5, S1-5 and Transparent methods. List of primary and secondary antibodies used in this study.

Gene	Forward (5' - 3')	Reverse (5' - 3')
CA2	TGTGCAGCAACCTGATGGACTG	ATCCAAGGATTCAGGAAGGAGG
MCT1	CATGTATGGTGGAGGTCCTATC	CAGAAAGAAGCTGCAATCAAGCC
MCT4	TTTTGCTGCTGGGCAACTTCTTCTG	TCACGTTGTCTCGAAGCATGGGTTT
PFKFB3	TGTTCAACGTGGGGAGTAT	GCAGCTAAGGCACATTGCTT

Table S3. Related to Figures 3, S3 and Transparent methods. List of primers used in this study.

TRANSPARENT METHODS

Cell Culture. U2OS and HeLa cell lines were purchased from American Type Culture Collection. Stable ER-E2F1 U2OS cell line was previously established in our laboratory (Real et al., 2011). Cell lines were cultured in DMEM high glucose with 4 mM L-Glutamine and 1 mM Pyruvate (Gibco) supplemented with 10% heat-inactivated fetal bovine serum (FBS) (Sigma Aldrich).

Reagents and chemicals. 4-hydroxytamoxifen (OHT) at 400 nM (Calbiochem), RAD001 at 5 nM (DELTACLON), BEZ235 at 50 nM (NOVARTIS), 3PO at 25 ☐M (MERCK), Oligomycin A at 1 mM (SIGMA) and 2DG at 50 mM or 100 mM (SIGMA). For all treatment conditions the control cells were treated with the corresponding vehicle.

Transfections: DNA transfection was performed following manufacturer's instructions using Lipofectamine 2000 (Life Technologies) in 1:5 Opti-MEM: DMEM medium. PFKFB3 (uPFK-2) expression vector was kindly provided by Dr. Ramon Bartrons (Duran et al., 2008), TIGAR plasmid was provided by Dr. Karen Vousden (Bensaad et al., 2006), ER-E2F1 expression vector was provided by Dr. Kristian Helin (Agger et al., 2005) and PFKP-EGFP was kindly shared by Dr. Bradley Webb (Webb et al., 2017). LAMP1-mRFP-Flag (#34611) plasmid was purchased in Addgene repository.

siRNA transfections were performed following manufacturer's instructions in Opti-MEM medium (Life Technologies) using Lipofectamine RNA-iMAX (Life Technologies). Unless otherwise indicated, siRNA transfections were performed for 48 hours. siRNA sequences and concentrations used in these studies are listed in Table S1.

Cell lysis and immunoblot analysis. Protein extraction, separation and detection were performed largely as described before (Meo-Evoli et al., 2015). Briefly, cells were lysed on Lysis Buffer [20 mM Tris-HCl pH 8, 10 mM EDTA, 150 mM NaCl, 1% Triton-X100] supplemented with protease inhibitors (Sigma-Aldrich) and phosphatase inhibitors cocktail 2 and 3 (Sigma-Aldrich). Protein concentration was analyzed using Pierce BCA Protein Assay kit (Thermo Fisher Scientific) following manufacturer's instructions.

Membranes were blocked with 5% non-fat dry milk in Tris-buffered saline containing 0.1% Tween-20 (TBS-T). Incubation of primary antibodies was performed overnight at 4ºC in 5% non-fat dry milk or 3.5% BSA (Sigma-Aldrich) in TBS-T solution. Used antibodies are listed in Table S2. Quantification of band intensities by densitometry was carried out using FIJI software (NIH).

Cross-linking and immunoprecipitation. After treatment, Rag B-FLAG ER-E2F1 stable U2OS cells were washed twice with ice-cold PBS. Cross-linking was performed by incubating cells with 1 mM dithiobis (succinimidyl propionate) (DSP) cross-linker reagent (Thermo Scientific) in PBS supplemented with protease and phosphatase inhibitors for 7 minutes at room temperature. 1 M Tris-HCl (pH 7.5) was added 1:10 to quench DSP activity for 5 minutes at room temperature. After cross-linking, cells were washed with ice-cold PBS and lysed in ice-cold IP-RIPA buffer [150 mM NaCl, 50 mM HEPES (pH 7.4), 1 mM EDTA, 1% NP-40, 1% sodium deoxycholate, 0.1 % SDS] supplemented with 2x protease and phosphatase inhibitors cocktails. Collected samples were centrifuged at 13,000 rpm for 5 minutes at 4 ºC and soluble fraction was subjected to BCA Pierce protein quantification. 500-1,000 µg of each lysate were separated for immunoprecipitation at 1 µg/µl concentration. For the immunoprecipitation, 20 µl of 50% slurry of anti-FLAG M2 beads were added to each lysate and incubated by rotation 2 hours at 4 ºC. Immunoprecipitates were washed three times with high salt RIPA [500 mM NaCl, 50 mM HEPES (pH 7.4), 1 mM EDTA, 1 % NP-40, 1 % sodium deoxycholate, 0.1 % SDS] and once with IP-RIPA. Immunoprecipitated proteins were denatured by the addition of 2X sample buffer followed by boiling for 10 minutes, resolved by 4 %-20 % Criterion TGX Gel (BIO-RAD) electrophoresis and analyzed by immunoblotting. 20 µg of the total lysate were loaded as input to control.

Quantitative real-time PCR (quantitative RT-PCR). Total RNA was extracted using TRIzol (Invitrogen) following manufacturer's instructions.1 µg of total RNA was subjected to reverse transcription and resulting cDNA samples were used (diluted 1:100) in PCR

amplification using LightCycler 96 SYBR Green I Master Mix (Roche Molecular Systems). Used sequences are listed in Table S3. Gene expression was normalized to the endogenous β-actin.

Metabolic assays. U2OS cells were seeded at optimal confluence of 700,000 cells per well. Measurements from pre-treated U2OS cells were performed using a XF24-Extracellular Flux Analyzer (Seahorse Bioscience) following standard Glycolysis Stress Test. Reagent's concentrations were optimized for U2OS cells. XF-Extracellular Flux Analyzer injection ports were used to inject assay reagents. Extracellular acidification rate (ECAR) was measured in unbuffered DMEM supplemented with 2 mM Glutamine. U2OS cells were starved of glucose for 1 hour prior to experiment followed by the addition of 25 mM D-glucose, 1 mM of Oligomycin A and 100 mM of 2DG. The protein concentration was determined by BCA Pierce and used to normalize the results.

Immunofluorescence analysis. Cells were plated onto glass coverslips and procedure was achieved as described before (Real et al., 2011). mTOR 1/100 (Cell Signaling, #2983) and LAMP2 1/300 (CD107b) (BD Biosciences #555803) primary antibodies were used for co-localization analysis. Anti-Mouse Alexa Fluor 488 and Anti-Rabbit Alexa Fluor 555 (Invitrogen) were used at 1/400 dilution. Fluorescence was detected with the Leica spectral confocal microscope TCS SP5 using a 63X N.A 1.4 objective and LAS AF software. Fluorophores were excited with Argon laser for 488 nm, DPSS 561 for 555 nm and Diode laser for 405 nm. Images were analyzed with FIJI software (NIH).

For lysosomes localization, individual cells were analyzed based on actin cytoskeleton and the distance between each lysosome and nucleus center was calculated using the pixels coordinates. Data from each cell was introduced to Prism4 software to process and obtain the corresponding plot. For co-localization coefficient, images were acquired using fixed settings and analyzed using ZEN software. Thresholds for the red and green

channels were adjusted and maintained during all the analysis. Percentage of red-green overlapping pixels over total red pixels was calculated.

Live-cell time-lapse videos. U2OS ER-E2F1 transiently expressing LAMP1-mRFP and PFKP-EGFP cells were grown onto glass bottom 8-well slides (IBIDI). Live-cell imaging was performed on the Leica spectral confocal microscope TCS SP5. Images were taken every 0.23 seconds for a total time of 10 minutes using the 63x glycerol objective.

Ultra Performance Liquid Chromatography (UPLC). U2OS cells were treated and harvested in triplicate. Cells were rinsed twice in cold PBS and collected in 400 µL of perchloric acid 2 M followed by incubation for 15 minutes at 4ºC. Supernatants were used for nucleotide measurement and pellets for protein determination. 100 µL of Bicine 1 M and 100 µL K_2CO_3 4 M were added to the supernatants. Nucleotide solution was subjected to vortex and centrifuged. The supernatant was frozen until UPLC analysis. For UPLC determination, samples were thawed and filtered using Nylon membrane 4 mm 0.45 µm Syring Filter (National Scientific). Samples were analyzed by UPLC on Acquity UPLC system with a Kinetex 2.6 µm C18000 Column (Phenomenex). Analyzes were performed using 15 µL sample injection volume at 35 ºC at a flow rate of 0.5 mL/min. Buffer A: MeOH 30%; Buffer B KH_2PO_4 0,05 M, 4 mM tetrabutyl ammonium hydrogen (TBA) pH=6 with 50% KOH. The UPLC program was: [0-5 min, 0% A; 5 min, 30% A; 10 min, 40% A; 19 min, 100% A; 22 min, 100% A; 23 min 0% A; 30 min, stop]. UV detection was set at 260 nM wavelength. Peaks were identified by retention times and compared to the peak spectrum of ATP/ADP/AMP standards. Area under the curve was analyzed using Empower Software (Waters) and values were normalized by protein amount.

Cytosolic pH measurement. Pre-treated U2OS cells were resuspended in PBS and incubated with 5 µM SNARF-AM for 30 minutes at 37 ºC. Samples were centrifuged, and the stained pellet was resuspended in PBS for flow cytometric analysis. pH extrapolation was performed using a standard curve from cells incubated at different pH, the protocol

used was as follows. After incubation with SNARF-AM and centrifugation, cells were resuspended in high potassium buffer [135 mM KH_2PO_4, 29 mM NaCl] supplemented with 10 µM Nigericin. Cell suspension was incubated for 20 minutes to equilibrate the intracellular pH and analyzed by flow cytometry. Bandpass filters were centered at 580 nm and 640 nm for ratio calculation.

Fructose 2,6-P_2 levels measurement. Samples were collected in extraction buffer [NaOH 100 mM; Triton X-100 0,1%], heated at 80 ºC for 20 minutes and centrifuged 15 minutes at 14,000 rpm, 15 minutes at 4ºC. Supernatant was collected and subjected to Bradford protein quantification (Bio-Rad). Then, supernatant was neutralized with acetate/acetic acid buffer 250 mM to pH 7-7.5. After a spin, supernatant was mixed with buffer reaction containing AUX, substrates (G6P and F6P), PFK1 and MiliQ water. Finally, PPi was added to the sample and Fructose 2,6-P_2 was quantified spectrophotometrically as previously described (Van Schaftingen et al., 1982).

Statistical analysis: Data was analyzed by GraphPad Prism4 software. Results are presented as Mean ± S.D., for n independent experiments. Experimental data-sets were compared by: (i) Two-sampled, two-tailed Student's t-test to compare two experimental conditions sharing normal distribution and variance (ii) One-way ANOVA test for more than 2 conditions sharing normal distribution. Multiple comparisons were corrected using Tukey's test for equal variances or using Dunett's T3 test for different variances. Statistical significance is shown as: * $p < 0.05$; ** $p < 0.005$; *** $p < 0.001$ for OHT effect compared to CTRL and # $p < 0.05$; ## $p < 0.005$; ### $p < 0.001$ for experimental condition compared to the respective control (CTRL condition A vs CTRL condition B and OHT condition A vs OHT condition B); ns: $p > 0.05$.